Physical Chemistry of Polymers: Entropy, Interactions, and Dynamics

T. P. Lodge*

Department of Chemistry and Department of Chemical Engineering & Materials Science, University of Minnesota, Minneapolis, Minnesota 55455

M. Muthukumar

Department of Polymer Science & Engineering and Materials Research Science and Engineering Center, University of Massachusetts, Amherst, Massachusetts 01003

Received: January 23, 1996; In Final Form: May 14, 1996[⊗]

A brief examination of some issues of current interest in polymer physical chemistry is provided. Emphasis is placed on topics for which the interplay of theory and experiment has been particularly fruitful. The dominant theme is the competition between conformational entropy, which resists distortion of the average chain dimensions, and potential interactions between monomers, which can favor specific conformations or spatial arrangements of chains. Systems of interest include isolated chains, solutions, melts, mixtures, grafted layers, and copolymers. Notable features in the dynamics of polymer liquids are also identified. The article concludes with a summary and a discussion of future prospects.

1. Introduction

1.A. General Remarks. Macromolecules form the backbone of the U.S. chemical industry, and are essential functional and structural components of biological systems.[1] Yet, the very existence of long, covalently bonded chains was in dispute only 70 years ago. The past 50 years has seen a steady growth in understanding of the physical properties of chain molecules, to the point that the field has achieved a certain maturity. Nonetheless, exciting and challenging problems remain. Polymer physical chemistry is a richly interdisciplinary field. Progress has relied on a combination of synthetic ingenuity, experimental precision, and deep physical insight. In this article, we present a brief glimpse at some interesting current issues and acknowledge some notable past achievements and future directions.

1.B. Basic Concepts. When N monomers join to form a polymer, the translational entropy is reduced. However, the entropy associated with a single molecule increases dramatically, due to the large number of different conformations the chain can assume.[2−11] Conformational changes occur at both local and global levels. Local conformational states with differing energies depend on the chemical nature of substituent atoms or side groups, X, as sketched in Figure 1. Typically, there are three rotational conformers at every C−C bond. These states, and the torsional energy as a function of rotation about the middle C−C bond, are represented in Figure 2. If $\Delta\epsilon \ll kT$, there exists complete static (i.e., equilibrium-averaged) flexibility. Even for higher values of $\Delta\epsilon/kT$, where the trans conformation is preferred, the chain will still be flexible for large N. We can define a statistical segment length, b, over which the local stiffness persists; b depends on the value of $\Delta\epsilon/kT$.[12] But, beyond this length, bond orientations are uncorrelated. The parameter which determines the overall chain flexibility is b/L, where L, the chain contour length, is $\sim N$. If $b/L \ll 1$, the chain has complete static flexibility; for $b/L \gg 1$, the chain is a rigid rod.

Similarly, $\Delta E/kT$ determines the dynamical flexibility. If $\Delta E/kT \ll 1$, the time $\tau_{seg} \sim \exp(\Delta E/kT)$ required for trans ↔ gauche isomerizations is short (i.e., picoseconds to nanoseconds in solution), and the chain is dynamically flexible. For higher values of $\Delta E/kT$, dynamical stiffness arises locally. However, for large scale motions, involving times much greater than τ_{seg}, the chain can still be taken to be dynamically flexible. The chemical details of the monomers and solvent affect the local properties, b and τ_{seg}. Macroscopic, or global, properties do

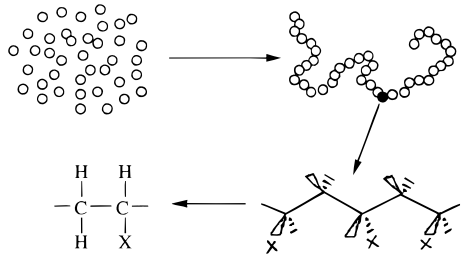

Figure 1. N monomers combine to form one linear chain, here with an all-carbon backbone and a pendant group denoted X.

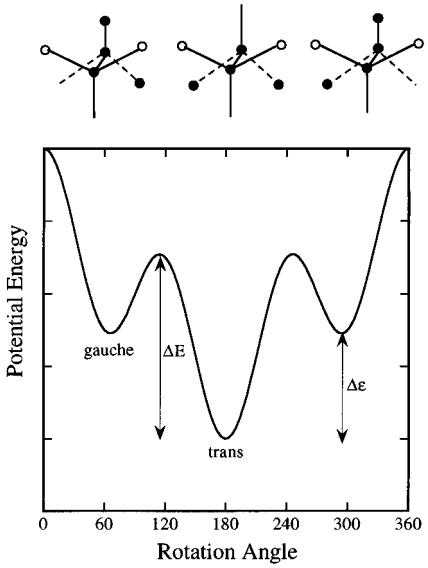

Figure 2. Schematic of the potential energy as a function of rotation about a single backbone bond and the corresponding trans and gauche conformers.

[⊗] Abstract published in *Advance ACS Abstracts,* July 15, 1996.

S0022-3654(96)00244-4 CCC: $12.00

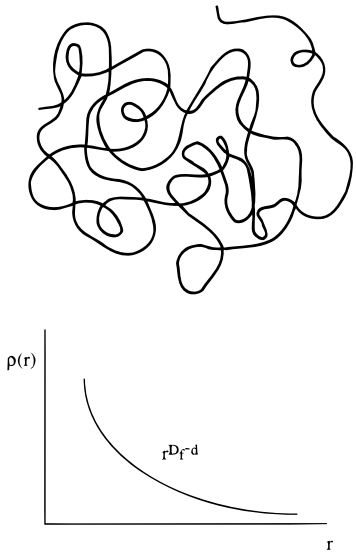

Figure 3. Schematic of a random coil polymer, and the density distribution $\rho(r)$ for $b \ll r \ll R_g$.

not depend directly on the local static and dynamic details and can be represented as universal functions (*i.e.*, independent of chemical identity) by "coarse-graining" the local properties into phenomenological parameters. Polymer physical chemistry deals with both the macroscopic properties, dictated by global features of chain connectivity and interactions, and the phenomenological parameters, dictated by the local details.

Connectivity leads to long-range spatial correlations among the various monomers, irrespective of potential interactions between monomers.[13,14] Such a topological connectivity leads naturally to statistical fractals,[15] wherein the polymer structure is self-similar over length scales longer than b but shorter than the size of the polymer. For the ideal case of zero potential interactions, the monomer density $\rho(r)$ at a distance r from the center of mass decays in three dimensions as $1/r$,[6,7] as shown in Figure 3. Consequently, the fractal dimension of the chain $D_f = 2$. This result is entirely due to chain entropy, but the long-ranged correlation of monomer density can be modified by potential interactions. In general, $\rho(r)$ decays as $(1/r)^{d-D_f}$, where d is the space dimension. Equivalently, the scaling law between the average size of the polymer, *e.g.*, the radius of gyration R_g, and N is $R_g \sim N^{\nu}$, where $\nu = 1/D_f$. The value of D_f is determined by the compromise between the entropy arising from topological connectivity and the energy arising from potential interactions between monomers. For example, most polymer coils with nonspecific short-ranged interactions undergo a coil-to-globule transition upon cooling in dilute solutions, such that the effective fractal dimension increases to about 3. Or, the chain backbone may be such that b increases at low T; in this case the chain can undergo a coil-to-rod transition, where D_f decreases monotonically to about 1. This competition between conformational entropy and monomer−monomer interactions represents a central theme of this article.

When specific, strong interactions such as hydrogen-bonding or electrostatic forces are present, chain conformations can suffer entropic frustration, as illustrated in Figure 4 for charge-bearing monomers.[16,17] In the process of forming the fully registered state (a) between the oppositely charged groups, the chain, via random selection, can readily form a topological state such as (b). The chain is entropically frustrated in state (b) since the two registered pairs greatly reduce the entropic degrees of freedom of the chain. The chain needs to wait until the pairs dissociate, accompanied by a release of entropy, and the process of registry continues. This feature of entropic frustration is

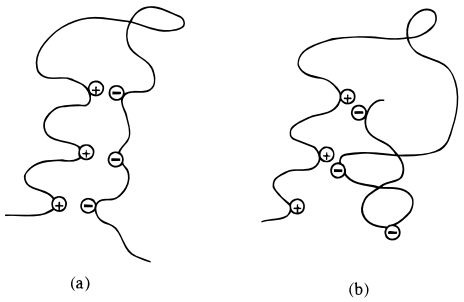

Figure 4. Illustration of (a) complete registry and (b) entropic frustration for a chain bearing both positive and negative charges.

common in macromolecules containing chemically heterogeneous subunits and in polymers adsorbing to an interface. When a chain is frustrated by topological constraints, not all degrees of freedom are equally accessible, and standard arguments based on the hypothesis of ergodicity may not be applicable. The identification of the resulting equilibrium structure is a challenge to both experiment and theory. The kinetics of formation of such structures is also complicated by the diversely different free energy barriers separating the various topological states. In general, the distance between different trajectories of the system diverges with time, and the presence of free energy minima at intermediate stages of evolution delays the approach to the final optimal state.[17] Several of these features are exemplified by biological macromolecules.

1.C. Recent Developments. *Synthesis.* Conventional polymerization methods, either of the step-growth (*e.g.*, polycondensation) or chain-growth (*e.g.*, free radical) class, produce broad molecular weight distributions and offer little control over long-chain architectural characteristics such as branching. Although of tremendous commercial importance, such approaches are inadequate for preparing model polymers, with tightly controlled molecular structures, that are essential for fundamental studies. For this reason, living polymerization has become the cornerstone of experimental polymer physical chemistry. In such a synthesis, conditions are set so that growing chain ends only react with monomers; no termination or chain transfer steps occur. If a fixed number of chains are initiated at $t = 0$, random addition of monomers to the growing chains leads to a Poisson distribution of chain length, with a polydispersity (M_w/M_n) that approaches unity in the high N limit. Block copolymers can be made by sequential addition of different monomers, branched chains by addition of polyfunctional terminating agents, and end-functionalized polymers by suitable choice of initiator and terminator. Examples of chain structures realized in this manner are shown in Figure 5.

The most commonly used technique, living anionic polymerization, was introduced in the 1950s.[18,19] It is well-suited to several vinyl monomers, principally styrenes, dienes, and methacrylates. However, it suffers from significant limitations, including the need for rigorously excluding oxygen and water, a restricted set of polymerizable monomers, and reactivity toward ancillary functionalities on monomers. Consequently, there is great interest in developing other living polymerization protocols.[20] Over the past 15 years, group transfer,[21] ring-opening and acyclic diene metathesis,[22−24] cationic,[25,26] and even free radical[27] living polymerization methods have been demonstrated. Soon a much broader spectrum of chemical functionalities will become routine players in the synthesis of model polymers, and commercial products will rely increasingly on controlled polymerization techniques.

Theory. The genesis of polymer theory is the realization that a conformation of a polymer chain can be modeled as the

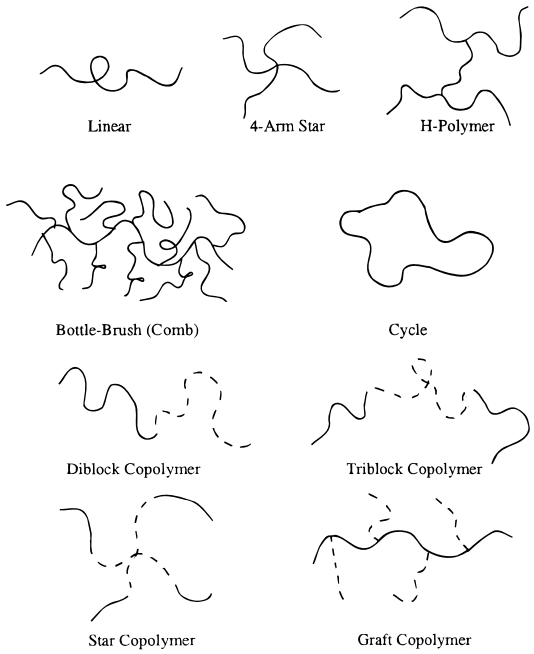

Figure 5. Various polymer topologies achieved by living polymerization techniques.

trajectory of a random walker.[2−11] In the simplest case, the apparent absence of any energy penalty for self-intersection, the statistics of random walks can be successfully applied. In the long-chain limit, the probability distribution $G(\vec{R},N)$ for the end-to-end vector of a chain, $\vec{R}$, is Gaussian, under these (experimentally realizable) "ideal" conditions. Now G satisfies a simple diffusion equation, analogous to Fick's second law:

$$\left(\frac{\partial}{\partial N} - \frac{b^2}{6}\frac{\partial^2}{\partial \vec{R}^2}\right)G(\vec{R},N) = \delta(\vec{R})\,\delta(N) \qquad (1.1)$$

Thus, N corresponds to time, G to concentration, and b^2 to a diffusivity. The right-hand side simply requires that the chain beginning at the origin arrive at $\vec{R}$ after N steps. When there is a penalty for self-intersections, due to excluded volume interactions between monomers, it is possible to compose a pseudopotential for segmental interactions. The diffusion equation now contains an additional potential term which, in turn, depends on G:[13,28]

$$\left(\frac{\partial}{\partial N} - \frac{b^2}{6}\frac{\partial^2}{\partial \vec{R}^2} + \frac{V[G(\vec{R})]}{kT}\right)G = \delta(\vec{R})\,\delta(N) \qquad (1.2)$$

This requires a self-consistent procedure to determine G, from which various moments of experimental interest can be derived; in essence, this process amounts to making an initial guess for G, calculating the potential term, and numerically iterating until the chosen G satisfies eq 1.2.

For multicomponent polymer systems, the local chemical details and the various potential interactions between effective segments can be parametrized by writing an appropriate "Edwards Hamiltonian" (see eq 2.1 and associated discussion).[7−9] Standard procedures of statistical mechanics (with varying levels of approximation) are then employed to obtain the free energy as a functional of macroscopic variables of experimental interest.[8,29−31] Such density functional approaches lead to liquid-state theories derived from coarse-grained first principles.[8] The free energy so derived, reflecting a quasi-microscopic description of polymer chemistry, is also used to access dynamics.

Simulation.[32,33] Lattice walks are used to determine G for a single chain with potential interactions, with some site potential energy to simulate chain contacts. A key feature of this approach is to use generating functions[34−37]

$$P(x) = \sum_{N=0}^{\infty} p_N x^N \qquad (1.3)$$

where p_N are probability functions describing chains of N steps; this greatly reduces the computational complexity. For fully developed excluded volume, the exact method enumerates all possible nonintersecting random walks of N steps on a lattice; assuming all configurations are *a priori* equally probable, various averages are then constructed. In the alternative Monte Carlo method, a chain of successively connected beads and sticks is simulated on various lattices, or off-lattice, and statistical data describing the chain are accumulated. The stick can be either rigid or a spring with a prescribed force constant; the latter case is referred to as the bond-fluctuation algorithm.[38] As before, the beads interact through an appropriate potential interaction. Once an initial configuration is created, a randomly chosen bead is allowed to move to a new position without destroying the chain connectivity. The energy of the chain in its new configuration is computed, and the move is accepted or rejected using the Metropolis algorithm.[39] Instead of making local moves, so-called pivot algorithms can be used to execute cooperative rearrangements.[40,41]

The use of molecular dynamics,[42] in which Newton's law is solved for the classical equation of motion of every monomer, has been restricted to rather short chains.[43,44] Such atomistic simulations are difficult for polymers since even a single chain exhibits structure from a single chemical bond (*ca.* 1 Å) up to R_g (*ca.* 10−10^3 Å), and the separation in time scale between segmental and global dynamics is huge. Brownian dynamics is an alternative method,[45] wherein Newton's equation of motion is supplemented with a friction term and a random force, which satisfy a fluctuation−dissipation theorem at a given T. Since the friction coefficient is in general phenomenological, this Langevin equation is usually written for an effective segment. All of the above methodologies are in current use.

Experimental Techniques. Polymers require a variety of techniques to probe their multifarious structures, dynamics, and interactions. Polymer structure may be probed in real space, by microscopy, and in Fourier space, by scattering. Both approaches are important, but scattering has been more central to the testing of molecular theory. Classical light scattering (LS) and small-angle X-ray scattering (SAXS) have been used for over 50 years, but small-angle neutron scattering (SANS) has, in the past 25 years, become an essential tool.[46−49] The key feature of SANS is the sharp difference in coherent scattering cross section between hydrogen and deuterium; isotopic substitution thus permits measurement of the properties of single chains, or parts of chains, even in the bulk state. All three experiments give information on the static structure factor, $S(q)$:

$$S(q) = \frac{1}{N^2}\sum_{j}^{N}\sum_{k}^{N}\langle \beta_j \beta_k^* \exp[-i\vec{q}\cdot(\vec{r}_j - \vec{r}_k)]\rangle \qquad (1.4)$$

where $\vec{q}$ is the scattering vector ($=(4\pi/\lambda)\sin(\theta/2)$, with λ the wavelength and θ the scattering angle). $S(q)$ generally contains both intramolecular ("form factor") and intermolecular ("structure factor") correlations and in the thermodynamic limit ($q \rightarrow 0$) measures the osmotic compressibility of the mixture. Consequently, scattering techniques provide valuable informa-

tion on molecular interactions, and not just structure. The accessible length scales depend on q and are typically $30-10^4$ nm for light, 0.5−50 nm for SANS, and 0.1−100 nm for SAXS. This combined range exactly matches that associated with macromolecular dimensions—monomer sizes on the order of 1 nm, molecular sizes up to 0.5 μm, and aggregates or multimolecular assemblies from 0.01 to 10 μm. The scattering power of individual monomers is embodied in the factor β_j, which depends on refractive index for LS, electron density for SAXS, and nuclear properties for SANS.

Polymers exhibit dynamics over many decades of time scale, ranging from segmental rearrangements in the nanosecond regime to long-range chain reorganizations that can take minutes or even days. Two classes of technique have proven particularly revealing in recent years: measurements of rheological properties and translational diffusion. The former concerns the response of a fluid to an imposed deformation; in the dynamic mode, the deformation is sinusoidal in time, and frequency variation permits investigation of different time scales of motion. Significant progress in commercial instrumentation has made these techniques accessible to a wide variety of researchers. The centrality of chain diffusion to the reptation model of entangled chain dynamics (*vide infra*) spurred an explosion of technique development and application in the late 1970s and 1980s, methods which are now being profitably applied to a much broader range of issues. Examples include forced Rayleigh scattering (FRS)[50] and forward recoil spectrometry (FRES);[51] more established methods, such as pulsed-field gradient NMR[52] and fluorescence photobleaching recovery,[53] also found many new adherents. Dynamic light scattering (DLS) has proven to be a particularly versatile and fruitful technique. It provides information on the dynamic structure factor, $S(q,t)$ (see eq 2.10 and associated discussion). Although most often applied to monitor mutual diffusion processes in solutions and blends, it can also reflect viscoelastic properties and conformational relaxation.[54−56]

The importance of the surface, interfacial, and thin film properties of polymers has encouraged application of surface-sensitive or depth-profiling techniques. Some of these are familiar to the analytical chemistry community—ESCA, SIMS, reflection infrared, and ellipsometry. Others, particularly X-ray and neutron reflectivity,[57,58] and the aforementioned FRES, are less familiar. As with SANS, neutron reflectivity exploits the scattering contrast between ^{1}H and ^{2}H to probe composition profiles normal to an interface, with spatial resolution below 1 nm. The wavevector dependence of the specular reflectance is sensitive to gradients of scattering cross section, even of buried interfaces, and for appropriate samples can provide a uniquely detailed picture of molecular organization. As with scattering methods in general, reflectivity suffers from the inversion problem: the absence of phase information means that one can never obtain a unique real-space transform from the data.

1.D. Brief Outline. For an article of this length, and a topic of this breadth, a good deal of selectivity is necessary. We have employed several criteria in this selection. First, we highlight areas that are of great current interest and in which substantial progress has been made in recent years. Some of these are "classical" issues (*e.g.*, excluded volume, chain entanglement) which have been examined for over 50 years, whereas others (*e.g.*, polymer brushes, copolymer phase diagrams) are of more recent vintage. Second, we emphasize phenomena which illustrate the concepts identified in section 1.B; some important problems which are not inherently polymeric (*e.g.*, the glass transition) are omitted. Third, and most important, we feature problem areas in which the interplay of theory and experiment has proven to be particularly fruitful.

Necessarily there is a great deal of personal taste, some might say arbitrariness, to the selection. Certainly there are serious omissions, both in topical coverage and in thorough referencing. For example, liquid crystalline polymers, polymer crystallization, polymers with interesting electrical and optical properties, polymer gels, and networks are all neglected. In the interests of clarity and simplicity, there are many issues for which the discussion is overly simplified. For all these sins and more, we can only apologize in advance.

In the next section, we consider the equilibrium and dynamic properties of isolated chains and then proceed to concentrated solutions, melts, and mixtures in section 3. In section 4 interfacial polymer systems are considered: polymer brushes, block copolymers, and micelles. We conclude with a brief summary and a discussion of possible future directions.

2. Dilute Solutions

2.A. Equilibrium. The probability distribution function $G(\vec{R},L)$ of the end-to-end vector $\vec{R}$ of an isolated chain with interactions can be expressed by the path integral[13]

$$G(\vec{R},L) = \int_{\vec{r}(0)}^{\vec{r}(L)} \mathrm{d}[\vec{r}]\, \exp\left\{ -\frac{d}{2b}\int_0^L \mathrm{d}s \left(\frac{\partial \vec{r}}{\partial s}\right)^2 - \frac{1}{2}\int_0^L \mathrm{d}s \int_0^L \mathrm{d}s'\, V[\vec{r}(s) - \vec{r}(s')] \right\} \quad (2.1)$$

where $\vec{r}(s)$ is the position vector of the sth monomer in d-dimensional space; $\mathrm{d}[\vec{r}]$ implies summation over all possible paths between the ends of the chain $\vec{r}(0)$ and $\vec{r}(L)$, and V is the potential interaction between the sth and s'th monomers. The argument of the exponential is referred to as the Edwards Hamiltonian; the first term, the "kinetic energy", reflects the chain conformation, while the second, the "potential energy", accounts for the energetics of monomer−monomer interactions. Usually it suffices to assume that V is short-ranged and is represented by a pseudopotential of strength w, $V = w\delta^d[\vec{r}(s) - \vec{r}(s')]$, where δ^d is the d-dimensional delta function. The excluded volume parameter, w, can be viewed as the angular-averaged binary cluster integral for a pair of segments:[5,7]

$$wb^2 = \langle \int \mathrm{d}[\vec{r}(s) - \vec{r}(s')]\{1 - \exp(-V)\}\rangle \quad (2.2)$$

Clearly w depends on T and on the (nonuniversal) specifics of the polymer and solvent. It is possible to define a special temperature, Θ, in the vicinity of which

$$w \sim (T - \Theta)/T \quad (2.3)$$

This Flory theta temperature[2] is somewhat analogous to the Boyle point of the van der Waals gas, in that it represents the temperature at which excluded volume repulsions and monomer−monomer attractions cancel, and the osmotic second virial coefficient vanishes. It is also the critical temperature for liquid−liquid phase separation in the infinite N limit. Consequently, both "upper" (*i.e.*, UCST) and "lower" (*i.e.*, LCST) theta temperatures are possible, although the former is much more common. At $T = \Theta$, $w = 0$ and $G(\vec{R},L)$ reduces to a Gaussian distribution. For this case, the mean-square segment-to-segment distance between segments i and j is proportional to $|i - j|$, so that $R_g \sim N^{1/2}$.[59]

If $w > 0$, monomer−monomer interactions are effectively repulsive, and the chain expands. Dimensional analysis of the Edwards Hamiltonian shows that the free energy is of the form[6]

$$\frac{F}{kT} \sim \frac{R_g^2}{L} + \frac{wL^2}{R_g^d} \tag{2.4}$$

with the first term reflecting the conformational entropy and the second the interactions. Since in the absence of excluded volume effects $R_g \sim L^{1/2}$, the appropriate dimensionless coupling constant is $z = wL^{(4-d)/2}$.[5,8] Therefore, R_g may be written as $L^{1/2}\alpha(z)$, where the expansion factor, $\alpha(z)$, needs to be determined. By minimizing F with respect to R_g, one obtains $R_g \sim L^{\nu}$, with $\nu = 3/(d+2)$. More rigorous derivation shows this exponent to be correct, in the asymptotic limit of $z \rightarrow \infty$, except for $d = 3$, where $\nu \approx 0.588$, not $^3/_5$.[8,60,61] The crossover formulas for R_g have been derived for arbitrary values of z between 0 and ∞,[8,11,60−62] in agreement with many experimental data.[63]

For $T \leq \Theta$ the chain shrinks and eventually undergoes a coil-to-globule transition.[8,64−66] It is now necessary to include three-body potential interactions in the Edwards Hamiltonian, where v is the new parameter:

$$G(\vec{R},L) = \int_{\vec{r}(0)}^{\vec{r}(L)} d[\vec{r}\,] \exp\left\{ -\frac{d}{2b}\int_0^L ds \left(\frac{\partial \vec{r}}{\partial s}\right)^2 - \frac{w}{2}\int_0^L ds \int_0^L ds'\, \delta^d[\vec{r}(s) - \vec{r}(s')] - \frac{v}{2}\int_0^L ds \int_0^L ds' \int_0^L ds''\, \delta^d[\vec{r}(s) - \vec{r}(s')][\vec{r}(s') - \vec{r}(s'')] \right\} \tag{2.5}$$

The free energy can be written ($d = 3$)

$$\frac{F}{kT} \sim \frac{R_g^2}{L} + \frac{wL^2}{R_g^3} + \frac{vL^3}{R_g^6} \tag{2.6}$$

For asymptotically large $|z|$, α is inversely proportional to $|z|$. Thus, a plot of $\alpha|1 - \Theta/T|\sqrt{M}$ versus $|1 - \Theta/T|\sqrt{M}$ should be linear as $T \rightarrow \Theta$ and constant for $T/\Theta \gg 1$, as illustrated for polystyrene/cyclohexane in Figure 6.[67,68]

The stiffness of the polymer backbone may be addressed by calculating explicitly the torsional energies associated with rotations about C−C bonds as functions of torsional angle and by calculating how far chain orientation persists along the chain contour. The rotational isomeric state model,[3,4] which is equivalent to a one-dimensional Ising model, permits exact calculations in the absence of any long-range correlations along the backbone. The key result, that the molecule is rod-like if the chain is sufficiently stiff, is physically apparent. Effective size exponents, ν_{eff}, can be ascribed to semiflexible chains in dilute solutions. As the temperature is lowered, ν_{eff} changes continuously from about $^3/_5$ to 1. Instead of possessing uniform curvature along the chain contour, there are several polymers where many rod-like regions, interspaced by coil-like regions, are formed. The formation of rod-like regions is a cooperative phenomenon and can appear as an abrupt change from a coil to a "helix" or rod configuration as the temperature is lowered; this is referred to as the helix−coil transition, although it is not a true phase transition.[69]

Chain stiffness can also arise from charged monomers. The size of a polyelectrolyte chain in solution has been studied extensively, but the experiments are difficult and not yet definitive, as recently reviewed.[70] If the charge density on the polyelectrolyte chain is sufficiently high and the electrostatic interaction is unscreened, the chain is rod-like. Questions about the electrostatic persistence length induced by the presence of charges on the chain,[71] the extent of counterion condensation on the polyelectrolyte,[72] and the structure factor are abundant

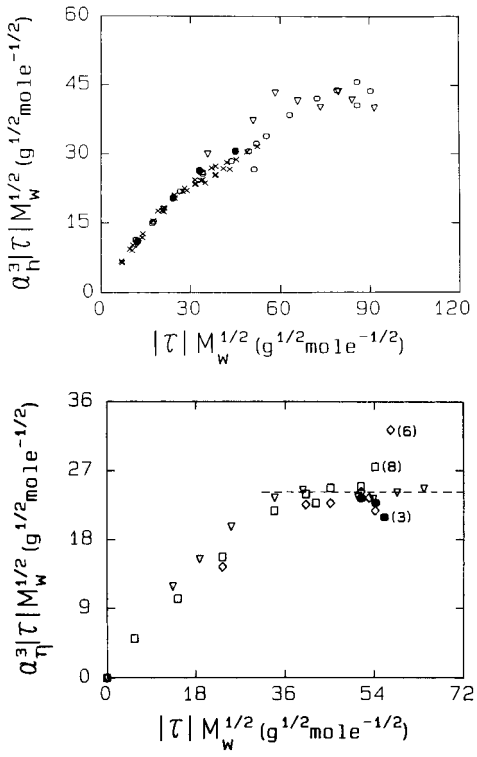

Figure 6. Coil-to-globule transition for polystyrene in cyclohexane; α_h and α_η denote the expansion factors obtained by dynamic light scattering and intrinsic viscosity, respectively, and $\tau = 1 - \Theta/T$.[67,68] The different symbols reflect measurements on different molecular weight samples. Reproduced with permission from refs 67 and 68.

in the literature.[70] To date, there is no completely satisfactory theory of polyelectrolytes. The theoretical description becomes ill-defined if the chain contains oppositely charged monomers or groups capable of undergoing specific interactions with each other. The origin of the difficulty lies in the entropic frustrations and accompanying issues of ergodicity. Such heteropolymers with prescribed sequences are excellent model systems to understand the more complex behavior of natural polymers like proteins and polynucleotides.

Many syntheses of linear polymers introduce chain branching as defects. In addition, certain branched polymers possess specific technological advantages over linear chains. Consequently, extensive research has been carried out in characterizing various branched polymers[73] such as stars, combs, randomly branched polymers, and dendrimers. For example, the ratio of the radius of a branched polymer to that of a linear polymer of the same total N is a function of the branching architecture. For a star polymer with f arms emanating from the center,

$$\frac{R_g^2(f)}{R_g^2(\text{linear})} = \frac{3f-2}{f^2} \tag{2.7}$$

in the absence of excluded volume effects.[74] Explicit expressions for other molecular architectures and the role of excluded volume are known.[5] In particular, the determination of the monomer density profile within a dendrimer has been of excitement,[75−79] due to the potential application of these molecules as uniquely functionalized, nanoscale closed interfaces.

2.B. Dynamics. The linear viscoelastic properties of isolated, flexible homopolymer chains are now almost quantitatively understood, at least for low to moderate frequencies, ω. The most successful framework for describing the dynamic shear modulus, $G^*(\omega)$, is the bead−spring model (BSM) of

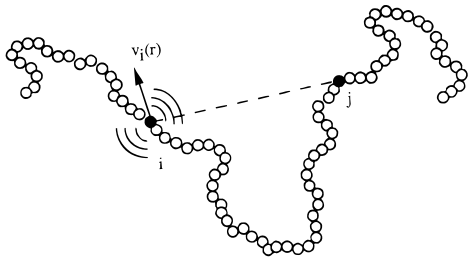

Figure 7. Illustration of hydrodynamic interaction: the motion of segment *i* perturbs the fluid velocity at all other segments *j*.

Rouse and Zimm,[80,81] wherein the chain is modeled as a series of $N + 1$ beads connected by N Hookean springs, embedded in a continuum of viscosity η_s.[7,82] The springs represent the entropic restoring force that resists chain extension or compression, while the beads provide friction with the solvent. The coupled equations of motion for the beads, in the (assumed) overdamped limit, relate the hydrodynamic, spring, and Brownian forces. Transformation to normal coordinates yields a series of N normal modes with associated relaxation times, τ_p. The longest relaxation time, τ_1, reflects the correlation time for fluctuations of the end-to-end vector (in both magnitude and orientation), whereas the progressively shorter relaxation times reflect motion of correspondingly smaller pieces of the chain. The dynamic shear modulus may be written

$$G^*(\omega) = \frac{cRT}{M}\sum_{p=1}^{N}\frac{\omega\tau_p}{1 + i\omega\tau_p} \tag{2.8}$$

The Zimm model differs from the Rouse treatment in its incorporation of intramolecular hydrodynamic interaction, in the preaveraged Kirkwood−Riseman approximation.[83] Physically, this corresponds to the through-space interaction between remote beads, which induces an additional cooperativity to the chain motion, as illustrated in Figure 7. Only the first "Oseen" or $1/r$ term is retained, and the preaveraging removes the dependence on the instantaneous positions of all the beads. For dilute solutions of flexible chains, incorporation of hydrodynamic interaction is essential for even qualitative agreement with experiment. The Rouse model is analytically soluble, however, whereas the Zimm model may only be solved numerically; exact eigenvalue routines are available.[84] Extensions to branched, cyclic, and copolymer chains have also been developed.[85−87]

A major limitation to the BSM is the omission of excluded volume forces. Consequently, it is most applicable to $T \approx \Theta$. However, excluded volume interactions have been incorporated approximately, via the bead distribution function employed in preaveraging the hydrodynamic interaction. Several approaches, including the renormalization group, have been shown to give almost indistinguishably successful fits to infinite dilution data.[87−89] However, one particularly appealing approximation is dynamic scaling, which asserts that, due to the self-similar nature of the chain conformation, all the relaxation times are related to the first through $\tau_p \sim \tau_1 p^{-3\nu}$, where $\tau_1 \sim R_g^3 \sim M^{3\nu}$.[7] From eq 2.8, one obtains the limiting behavior for $\omega\tau_1 \gg 1$ (but $\omega\tau_{seg} \ll 1$):

$$G' \sim (\omega\tau_1)^{1/3\nu}\frac{\pi}{6\upsilon}\frac{1}{\sin(\pi/6\nu)};\quad G'' \sim (\omega\tau_1)^{1/3\nu}\frac{\pi}{6\upsilon}\frac{1}{\cos(\pi/6\nu)} \tag{2.9}$$

The success of this approach is illustrated in Figure 8.[89]

The BSM is inadequate at high frequencies ($\omega\tau_{seg} \leq 1$), where details of the chemical structure intervene, and at higher rates of strain, where chain extensions become substantial. In the former, the assumption of the solvent as a continuum breaks down. Interesting manifestations of this include polymer-induced modification of the relaxation characteristics of the solvent,[90] negative intrinsic viscosities,[90] non-Kramers scaling of segmental motion with η_s (*e.g.*, $\tau_{seg} \sim \eta_s^{\alpha}$ with $\alpha < 1$),[91] spatial heterogeneity in the solvent mobility,[92] and apparent failures of time−temperature superposition.[93] Quantitative treatments of these phenomena remain elusive. At high strain rates the ubiquitous phenomenon of shear thinning, in which the steady-shear viscosity decreases with shear rate, is not captured by the simple BSM.[82] However, various enhancements (nonpreaveraged hydrodynamic interaction, nonlinear springs, *etc.*) show promise in this regard.[82]

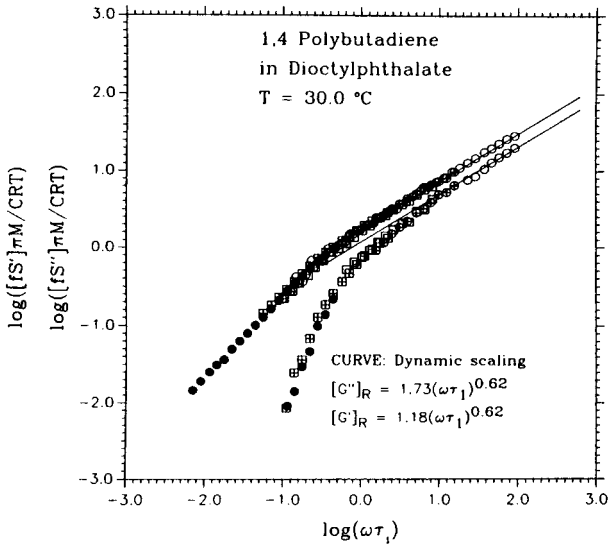

Figure 8. Infinite dilution shear moduli for polybutadienes in dioctyl phthalate, showing the success of dynamic scaling: the slopes, vertical separation, and absolute location of the curves are fixed for one value of $\nu = 0.538$. The data were acquired by oscillatory flow birefringence, and were converted to G' and G'' via the stress−optical relation; f is the frequency in hertz, M is the molecular weight, C is the stress−optic coefficient, and S' and S'' are the viscous and elastic components of the dynamic birefringence, respectively. Reproduced with permission from ref 89.

A full treatment of chain dynamics requires description not only of $G^*(\omega)$ but also of the dynamic structure factor, $S(q,t)$:

$$S(q,t) = \frac{1}{N^2}\sum_j^N\sum_k^N\langle\beta_j\beta_k^* \exp(-i\vec{q}\cdot[\vec{r}_j(t) - \vec{r}_k(0)])\rangle \tag{2.10}$$

This has been addressed via linear response theory.[54,94] Concurrently, extensive experimental results have become available, primarily through dynamic light scattering.[95] In essence, $S(q,t)$ monitors the spontaneous creation and relaxation of concentration fluctuations with wavelength $2\pi/q$. Three limiting regimes may be defined. For $qR_g \ll 1$, these fluctuations require molecular translation to relax, and $S(q,t) = S(q,0)\exp[-q^2Dt]$ for a monodisperse polymer, where D is the diffusion coefficient. In the Kirkwood−Riseman treatment, extended to non-theta solutions,

$$D = kT/6\pi\eta_s R_h \tag{2.11}$$

i.e., it follows the Stokes−Einstein equation with the hydrodynamic radius, R_h, appropriately defined ($R_h \sim R_g$). For $qb \approx 1$, the length scale of fluctuations corresponds to motion on the monomer scale. These may also be diffusive at short times but become subdiffusive when the chain connectivity is felt. This crossover has been accessed by neutron spin-echo spec-

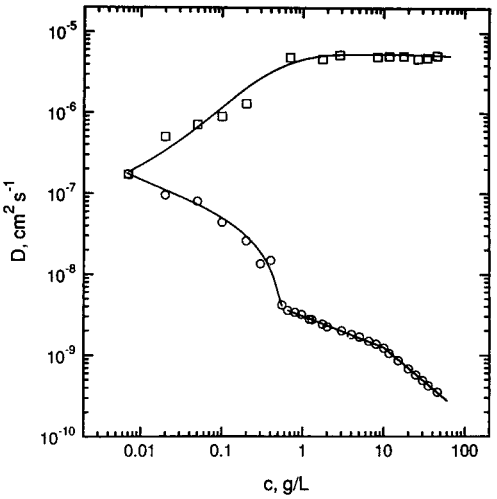

Figure 9. Fast and slow diffusion modes for a high molecular weight polystyrene sulfonate ($M_w = 1.2 \times 10^6$) in deionized water, measured by dynamic light scattering at a scattering angle of 90°. Reproduced with permission from ref 99. Copyright 1992 American Institute of Physics.

troscopy.[96] The intermediate regime, with $qR_g > 1$ and $qb < 1$, follows the internal modes of the chain. Here the Zimm theory predicts that $S(q,t)$ is a function of $t^{1/3\nu}$, which has been confirmed experimentally.[97] (Note the correspondence between this exponent and that for $G^*(\omega)$ when $\omega\tau_1 \gg 1$.) The first cumulant of $S(q,t)$, $\Omega(q)$ ($\equiv -\lim_{t\to 0}(1/S(q))(\partial S(q,t)/\partial t)$), displays a characteristic q^3 scaling, which may be understood quite simply. For internal modes, one expects Ω to be independent of M and a function of qR_g alone. The self-similarity of the chain implies that this be a homogeneous scaling function, $f(x)$, which reduces to unity as $qR_g \to 0$. Consequently, $\Omega = q^2Df(qR_g)$, and molecular weight independence imposes $f(x) \sim x$. (Note that the Rouse theory, with no hydrodynamic interactions, gives $f(x) \sim x^2$ and $\Omega \sim q^4$.) Linear response theory calculations of the ratio Ω/q^3 are found to be systematically in error by 10−15%, for reasons that are not fully apparent.[98]

The dynamics of polyelectrolyte solutions are considerably more complicated than those of homopolymers and not yet well understood; this is not surprising, given the recalcitrant difficulties in describing even the equilibrium properties. As an example, dynamic light scattering studies show that decreasing the salt concentration in solutions causes $S(q,t)$ to suddenly split into two modes, as illustrated in Figure 9.[99] This "ordinary−extraordinary transition" occurs at some critical salt concentration or at some polyelectrolyte concentration if the salt concentration is kept low.[100,101] This phenomenon is apparently universal and is observed in diverse polyelectrolyte systems including biopolymers. The faster mode is attributable to strong coupling between counterion and polyion motions.[99,102] The slower mode, however, remains rather mysterious, as it implies the existence of large domains or chain aggregates; these may be related to the observations that underlie speculation about long-range attractive forces in polyelectrolyte and colloidal solutions.[103]

3. Concentrated Solutions and Melts of Homopolymers

3.A. Homogeneous State: Chain Conformation. Consider a melt of flexible polymer chains. Although it might appear that many-body interactions would make this a much more complicated problem than dilute solutions, it is not so. Two great simplifications arise. First, in the melt chains adopt Gaussian conformations; according to the "Flory theorem", the intrachain excluded volume interactions are completely screened.[2,6]

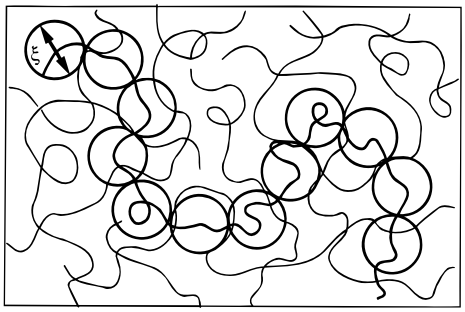

Figure 10. Illustration of the concept of a "blob", or correlation length, ξ, in a semidilute polymer solution.

Second, intramolecular hydrodynamic interactions are absent. Consequently, the Rouse description of chain dynamics becomes an excellent approximation, but only for short chains. A new phenomenon arises in the dynamics, however: chain entanglement.[104] The mutual uncrossability of long chains exerts a dramatic influence on the viscoelastic and diffusional properties of the molecules.

The screening of excluded volume interactions can be understood conceptually as follows. For a single chain in an athermal solvent, hard-core repulsive interactions between monomers cause the chain to swell beyond the random walk dimensions. In the melt, although the surroundings remain athermal, all monomers are indistinguishable. Thus, one monomer cannot tell whether a spatial nearest neighbor belongs to the same chain or not. Thus, swelling of the chain will not decrease the number of monomer−monomer contacts, and Gaussian statistics prevail. Although Flory first predicted this almost 50 years ago,[105] it was only the advent of SANS in the early 1970s that permitted testing of this proposition;[106] it has now been firmly established for many polymer systems.[107] Furthermore, the form factor of a single chain (for $qb < 1$) is given simply by the Debye function (the Fourier transform of the Gaussian distribution):

$$P(q) = \frac{2N}{q^4 R_g^4}(\exp[-q^2R_g^2] + q^2R_g^2 - 1) \qquad (3.1)$$

which plays a central role in the random phase approximation (RPA) formulation of $S(q)$ for polymer mixtures.[6] However, the conformation of a single chain in a melt of chains of varying molecular weights, or in miscible blends, has not been systematically explored.

For a polymer in a good solvent, excluded volume interactions become progressively screened as concentration increases. The coil overlap concentration, c^*, denotes the crossover between the dilute and semidilute regimes and may be estimated as

$$c^* \approx 3M/4\pi N_{av}R_g^3 \qquad (3.2)$$

Thus, coil overlap begins when the global polymer concentration equals the local average concentration within a single coil. In a semidilute solution, the interpenetrating chains may be considered to form a transient network, with a correlation length, or mesh size, ξ, as shown in Figure 10. On length scales shorter than ξ, excluded volume interactions are still felt, whereas for longer length scales the chains become indistinguishable. The concentration dependence of ξ may be obtained by a simple scaling analysis, assuming (a) ξ is independent of M, (b) $\xi = R_g$ when $c = c^*$, and (c) $\xi(c) = R_g f(c/c^*)$, where f is a homogeneous function. The result is $\xi \sim c^{\nu/(1-3\nu)}$. A sequence of monomers, g, corresponding to ξ is termed a "blob".[108] The polymer is viewed as a chain of blobs, with

$$R_g^2 \sim (N/g)\xi^2 \tag{3.3}$$

which leads to the prediction that R_g decreases as $c^{-1/8}$ in the good solvent semidilute regime. Some initial experiments were roughly consistent with this,[109] whereas others were not;[110] however, advances in both SANS and synthetic techniques suggest that this issue should be reexamined.

3.B. Homogeneous State: Chain Dynamics. The phenomenon of chain entanglement remains the central issue in polymer dynamics, although the past 20 years has seen a great deal of progress.[7,104,111] It is helpful to review the experimental manifestations of entanglement before considering possible molecular interpretations. Consider the time dependence of the stress relaxation modulus, $G(t) = \sigma(\tau)/\gamma$, after imposition of a step strain of magnitude γ at $t = 0$; a typical result for a high M melt is shown in Figure 11.[112] At very short times the magnitude of G is characteristic of a glass, and then relaxation occurs. This may be attributed to motion on the segmental level, *i.e.*, 1−50 monomers. However, at an M-independent characteristic time, τ_e, the relaxation virtually ceases, and $G(t)$ exhibits a plateau. Eventually, the relaxation resumes, and $G(t)$ decays to zero, as it must for a liquid. The "terminal" relaxation time, τ_1, associated with this flow regime, may be seconds or hours and depends strongly on M. The plateau region ($\tau_e < t < \tau_1$) may span several decades of time; its duration is a strong function of M. This feature is reminiscent of a cross-linked rubber, and indeed the (M-independent) magnitude of $G(t)$ in the plateau, designated G_N, is comparable to that for lightly cross-linked rubbers.[104] The standard interpretation is that the chains exhibit temporary cross-links, or entanglements, that inhibit long-range motion. Eventually, the chains must escape these constraints, and the liquid flows. Borrowing a formula from rubber elasticity,[113] $G \approx \rho RT/M_x$, where M_x is the M between cross-links, one can define an apparent M between entanglements, M_e, as $\rho RT/G_N$. Typically, M_e corresponds to 150−200 monomers. Other commonly invoked manifestations of entanglement are a plateau in $G'(\omega)$ (the cosine Fourier transform of $G(t)$), a strong increase in the M dependence of η, at a characteristic $M_c \approx 2M_e$ ($\eta \sim M$ for $M < M_c$ and $\eta \sim M^{3.4}$ for $M > M_c$), and the large scale elastic recovery of deformed polymer liquids.

A fundamental understanding of the entanglement phenomenon remains elusive. Although clearly intimately related to chain uncrossability, that is not sufficient; *n*-alkanes may not pass through one another, yet they do not entangle in this sense. The entanglement spacing does correlate well with the amount of chain contour per unit volume, and furthermore, the onset of entanglements (*i.e.*, $M = M_e$) corresponds roughly to the point at which the spherical volume pervaded by a test chain is also occupied by one other chain.[114,115]

The reptation model provides an appealingly simple picture of entangled chain motion[7,116] and makes predictions that are, in the main, in good agreement with experiment.[111] The entanglements are viewed as a quasi-permanent network, with a mesh size, $d \sim M_e^{1/2}$. Although local motions are isotropic, a chain can only escape the entanglements by diffusing along its own contour, like a snake, as illustrated in Figure 12. In the reptation time, τ_{rep}, the center of mass travels a root-mean-square curvilinear length, L, equal to $(M/M_e)d$. The friction experienced during this quasi-one-dimensional diffusion is assumed to be Rouse-like, *i.e.*, proportional to M. Thus, $\tau_{rep} \sim L^2(M/kT) \sim M^3$. During the same time interval, the center of mass moves in three dimensions an rms distance of order R_g, so that the diffusivity, D, scales as $R_g^2/\tau_{rep} \sim M^{-2}$. Prior to the reptation idea, there had been very few studies of chain diffusion. In recent years, however, an extensive body of data has been acquired, in general agreement with this prediction.[111] The rheological properties of polymer melts may also be predicted on the basis of reptation,[7] in partial agreement with experiment; a few discrepancies do remain. For example, theory predicts $\eta \sim \tau_{rep} \sim M^3$, whereas the exponent 3.4 ± 0.2 is universally observed.[104,117] Also, the exact shape of $G'(\omega)$ and $G''(\omega)$ in the terminal region is not well-captured by reptation, which is almost a single relaxation time process. One possible explanation is the presence of additional lateral degrees of freedom, due to the transient nature of the entanglements, that are not incorporated in the simple reptation picture.[118,119]

The reptation process on time scales shorter than τ_{rep} can also be explored.[7] Consider the mean-square displacement of an arbitrary monomer, $g(t) \equiv \langle[\mathbf{r}^2(t) - \mathbf{r}^2(0)]\rangle$. For very short times, a monomer is unaware of its connectivity, so $g(t) \sim t$. However, very soon it becomes aware of its bonded neighbors, and $g(t) \sim t^{1/2}$. This subdiffusive behavior is characteristic of a random walk of defects along the chain, which is a random

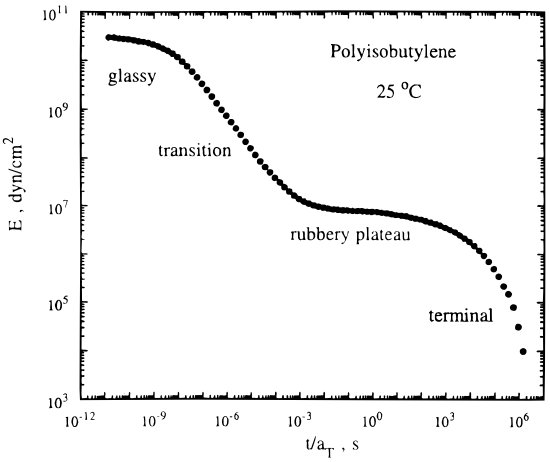

Figure 11. Relaxation modulus (obtained in extension, not shear) for high molecular weight polyisobutylene; original data of Tobolsky and Catsiff.[112] The data obtained at several temperatures have been reduced to one master curve by time−temperature superposition.

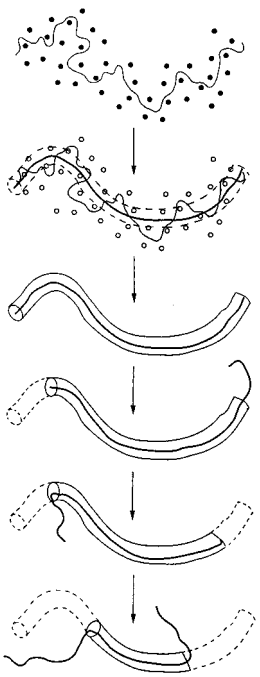

Figure 12. Replacement of a chain surrounded by entanglements by a snake in a tube, following Doi and Edwards;[7] the original tube is slowly "destroyed" as the chain escapes through the ends.

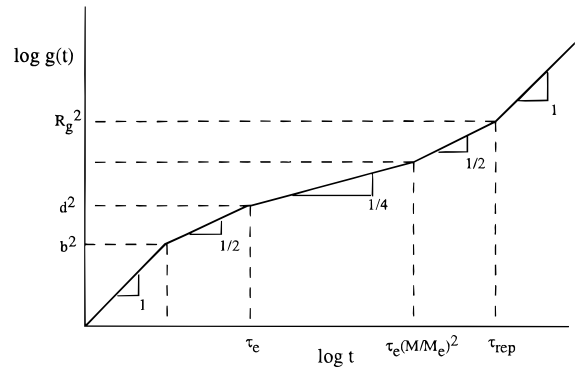

Figure 13. Time evolution of displacement for an arbitrary monomer on a reptating chain.[7]

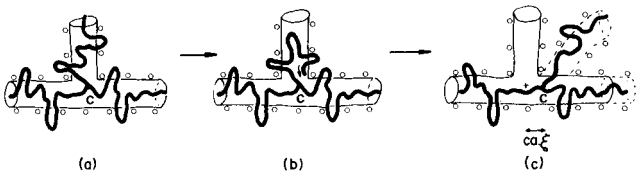

Figure 14. Diffusion of entangled three-arm star polymer by the arm-retraction mechanism, as illustrated by Klein. Reproduced with permission from ref 125.

walk itself. The scaling of r with $t^{1/4}$ is the exact analog of the $\Omega \sim q^4$ scaling for the internal modes of an isolated Rouse chain, mentioned in section 2. For an unentangled chain, $g(t)$ returns to Fickian behavior when the displacement exceeds R_g, as now all monomers move in concert with the center of mass. However, for a reptating chain, two new, subdiffusive regimes intervene, as shown in Figure 13. First, when the displacement is of order d (at time τ_e), the entanglement constraints further retard the spatial excursion of the chain, and $g(t) \sim t^{1/4}$. Then, on a time scale sufficient to allow defects to propagate along the chain length, $g(t)$ becomes Rouse-like again and scales as $t^{1/2}$. These various scaling laws have been energetically pursued, by both experiment[120,121] and simulation.[44,122] The results remain somewhat controversial, but the existence of an intermediate dynamic length scale, d, corresponding exactly to that associated with M_e from rheology, has been firmly established by neutron spin-echo measurements, and the character of the slowing down of $g(t)$ is in good agreement with reptation predictions.[121]

The dynamics of branched polymers of controlled architecture has also shed considerable light on the reptation model. For example, a three-armed star polymer cannot be expected to reptate.[118,123−125] If the arms are sufficiently entangled, the principal mode of relaxation is for the free end of arm to retract through the entanglements, as shown in Figure 14. This requires a random walk to retrace itself, which is exponentially unlikely: $\tau_{arm} \sim \exp(-M_{arm}/M_e)$. Considerable experimental evidence for this scaling has been accumulated, in both diffusion and viscosity.[111]

An extensive critical comparison of reptation predictions with experiment has been given,[111] and as mentioned above, the results are on the whole extremely good. Why, then, is the reptation picture still controversial? There are several difficulties. First, the reptation model is that of a single chain in a mean field, and it is doubtful how well this can capture what is so inherently a many-chain effect. Second, the reptation model says nothing about what entanglements are; it assumes their existence as a first step. Third, it is a hypothesis for the predominant chain motion, rather than the result of a microscopic theory. There has emerged no microscopic basis for reptation. Rather, it has been shown that a variety of other physical pictures can lead to comparable phenomenology.[126−129] In particular, the mode-coupling approach has been able to capture most of the same predictions, without any preference for longitudinal chain motion.[128] It is possible, therefore, that the observed scaling laws are more a consequence of long-range spatial correlations in the dynamics than of any particular mode of motion. This area is likely to remain fruitful, at least on the theoretical side; experimentally, one could argue that sufficient data exist to test any model thoroughly. The key for any new model is to make testable predictions that are qualitatively different from reptation.

Chain dynamics in nondilute solutions are more complicated than in either dilute solutions or melts. The reasons for this are several. First, there is a progressive screening of intramolecular hydrodynamic interactions as concentration increases, resulting in a broad crossover from Zimm-like to Rouse-like behavior in the vicinity of, or above, c^*. Second, at a concentration, c_e, that usually falls between $2c^*$ and $10c^*$, the onset of entanglement effects becomes apparent for high molecular weight chains. Third, the progressive screening of excluded volume interactions leads to a gradual contraction of average chain dimensions. Fourth, the concentration scaling laws that work rather well for static properties such as ξ do not hold as well for the dynamic screening length. Fifth, the local friction coefficient, ζ ($\sim\tau_{seg}$), is an increasingly strong function of concentration, particularly for polymers such as polystyrene with a glass transition well above room temperature. Consequently, interpretation of data in this regime remains controversial; for example, the same results have been advanced as evidence both for and against the onset of reptative motion.[111]

3.C. Phase Behavior. A standard method of making new materials is blending. In general, polymers do not mix well, for reasons discussed below. The continuing demand for new materials has forced a deeper examination of the factors which control polymer miscibility. Most of the essentials are contained in the simplest theory of polymer thermodynamics, due to Flory and Huggins.[2,130] Consider a blend of n_1 chains of type 1 each with N_1 segments and n_2 chains of type 2 each with N_2 segments. Let ϵ_{11}, ϵ_{22}, and ϵ_{12} be the energies of interaction associated with 1−1, 2−2, and 1−2 contacts. Assuming random mixing, which (incorrectly) disregards any topological correlation associated with chain connectivity, the free energy of mixing per unit volume is

$$\frac{F}{kT} = \frac{\phi_1}{N_1}\ln\phi_1 + \frac{\phi_2}{N_2}\ln\phi_2 + \chi\phi_1\phi_2 \qquad (3.4)$$

where the volume fraction of component i is $\phi_i = n_iN_i/(n_1N_1 + n_2N_2)$ and $\chi = (z/2kT)[2\epsilon_{12} - \epsilon_{11} - \epsilon_{22}]$, with z being the effective coordination number. At this level of approximation, the (nonuniversal) $\chi \sim T^{-1}$.

The Flory−Huggins theory is exactly equivalent to regular solution theory and the Williams−Bragg theory of metal alloys.[131] Standard thermodynamic analysis[132] locates the critical point

$$\chi_c = \frac{1}{2}\left(\frac{1}{\sqrt{N_1}} + \frac{1}{\sqrt{N_2}}\right)^2; \quad \phi_{1c} = \frac{\sqrt{N_2}}{\sqrt{N_1} + \sqrt{N_2}} \qquad (3.5)$$

with critical exponents that are mean-field-like. The entropy of mixing for polymers scales as N^{-1} and is consequently very small; thus, even small heats of mixing are sufficient to render polymer pairs immiscible. The scaling of T_c with N^{-1} has only recently been confirmed experimentally.[133] For $T < T_c$, *i.e.*, $\chi > \chi_c$, there is a range of compositions where the system is

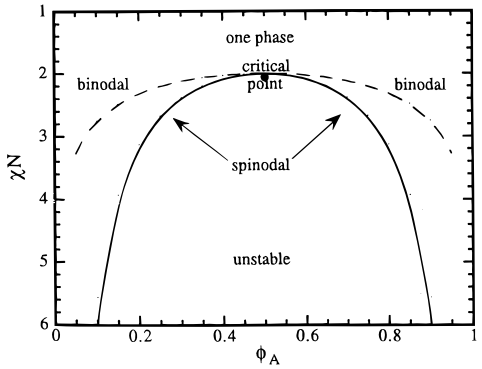

Figure 15. Phase diagram for a symmetric polymer blend ($N_1 = N_2$), according to the Flory−Huggins theory.

thermodynamically either unstable or metastable. The coexistence curve (binodal) depicting the compositions of coexisting phases at different temperatures is obtained by the thermodynamic stipulation that the chemical potential of every component is the same in all coexisting phases. The spinodal curve, which separates the region of thermodynamic instability from this region of metastability, is obtained by

$$A = \frac{\partial^2(F/kT)}{\partial {\phi_1}^2} = \frac{1}{N_1\phi_1} + \frac{1}{N_2\phi_2} - 2\chi = 0 \qquad (3.6)$$

The resulting UCST phase diagram is illustrated in Figure 15.

Defining an order parameter $\psi = \phi_1 - \phi_{1c}$, the Flory−Huggins free energy, upon Taylor series expansion in ψ, leads to the Landau expansion

$$\frac{F}{kT} = \frac{F_0}{kT} + \frac{A}{2}\psi^2 + \frac{B}{4}\psi^4 \ldots \qquad (3.7)$$

where F_0 is a constant. As $T \rightarrow T_c$, $A \rightarrow 0$, so that F is sensitive to ψ only through the quartic term. This indicates that there is an increase in fluctuations in ψ as $T \rightarrow T_c$, *i.e.*, local inhomogeneities are created spontaneously. This expansion can be generalized to the inhomogeneous case by the Landau−Ginzburg free energy

$$\frac{F}{kT} = \int \frac{d^3\vec{r}}{V}\left[\frac{F_0}{kT} + \frac{A}{2}\psi^2(\vec{r}) + \frac{B}{4}\psi^4(\vec{r}) \ldots + \frac{\kappa}{2}(\nabla\psi)^2 + \ldots\right] \qquad (3.8)$$

where $\psi(\vec{r})$ is now position-dependent. The square-gradient Ginzburg or Cahn−Hilliard term[134] depicts the free energy penalty associated with the creation of interfaces.

The coefficient κ dictates the interfacial tension, Γ, and the interfacial width, λ, between the two coexisting phases:

$$\Gamma \sim kT_c\sqrt{\kappa}\frac{|A|^{3/2}}{B}; \quad \lambda \sim \sqrt{\kappa/|A|} \qquad (3.9)$$

For polymer blends, creation of interfaces at length scales shorter than R_g requires conformational distortion of the chains. Such entropic contributions to κ dominate the usual enthalpic terms arising from potential interactions between segments; the latter are the only factor for small molecules. Using a mean-field theory for such entropic fluctuations, called the random phase approximation (*viz.*, the collective density modes are decoupled),[6] the (N-independent) κ becomes

$$\kappa = \frac{1}{3}\left(\frac{{R_{g1}}^2}{N_1\phi_1} + \frac{{R_{g2}}^2}{N_2\phi_2}\right) \qquad (3.10)$$

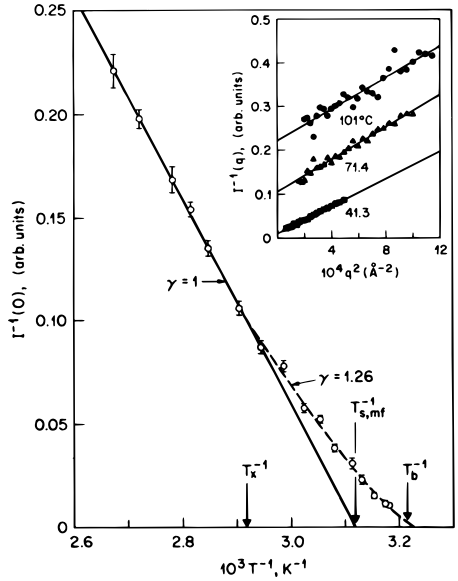

Figure 16. Mean-field to Ising-like crossover in the inverse intensity for a polyisoprene−poly(ethylenepropylene) blend. Reproduced with permission from ref 137. Copyright 1990 American Institute of Physics.

The change in free energy to excite a fluctuation, $\Delta\psi = \psi - \psi_0$, where ψ_0 is the equilibrium value, is

$$\frac{F}{kT} = \int \frac{d^3\vec{r}}{V}\left[\frac{A}{2}(\Delta\psi)^2 + \ldots + \frac{\kappa}{2}(\nabla(\Delta\psi))^2 + \ldots\right] \qquad (3.11)$$

Therefore, the static structure factor, $S(q)$, which is the Fourier transform of the mean-square fluctuations, follows the Ornstein−Zernicke form

$$S(q) = \langle|\Delta\psi(q)|^2\rangle = \frac{1}{A}\frac{1}{1 + q^2\xi^2} \qquad (3.12)$$

where the correlation length $\xi = \sqrt{(\kappa/A)}$. The scattered intensity $I(q)$ ($\sim S(q)$) as a function of ϕ and T determines A and ξ. As $T \rightarrow T_s$, $I(0)$ and ξ diverge as $|T - T_s|^{-\gamma}$ and $|T - T_s|^{-\nu}$, respectively, where the mean-field exponents are $\gamma = 1$ and $\nu = {}^1/_2$.

Critical phenomena of polymer blends fall in the same universality class as the d = 3 Ising spin system, where $\gamma = 1.26$ and $\nu = 0.63$, as shown by voluminous experimental data on different small molecular mixtures, spin systems, and renormalization group calculations.[135] Therefore, these Ising values should be observed for polymer blends near T_c. However, polymer blends are expected to be more mean-field-like, for the following reason. The mixing entropy is $\sim N^{-1}$ and the enthalpy is $\sim\chi$; therefore, the key experimental variable is χN. This is equivalent to the statement that the coordination number is zN, which is very large; thus, mean-field theory is more applicable. A Ginzburg criterion for polymer blends can be constructed to find the experimental range of applicability of mean-field theory.[136] Yet, as one approaches T_c closely enough, there is a crossover between mean-field to Ising behavior, as shown in Figure 16.[137−139]

Equation 3.4 fails to provide a quantitative description of real polymer mixtures. This is not particularly surprising, given its underlying simplicity. It is common practice to use eq 3.4 or 3.6 with χ as a fitting function; χ thus defined incorporates the excess thermodynamic functions and often depends on N and ϕ. Furthermore, χ always exhibits a temperature-independent "entropic" component that is often dominant. This term is present even for isotopic blends.[140] A full molecular theory

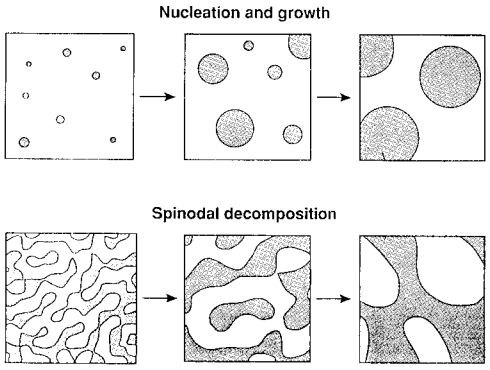

Figure 17. Schematic illustration of phase separation by nucleation and growth and by spinodal decomposition.

for this χ function would be extremely useful, but probably unwieldy. Given that $(\chi N)_c \approx 2$, for $N = 10^3$ one would require accuracy in χ to the fifth decimal place, *i.e.*, knowledge of the interactions at the level of $10^{-5}kT$. It is also the case that most miscible blends exhibit a negative χ; *i.e.*, specific interactions drive mixing. These systems usually display LCST behavior (demixing upon heating) due to compressibility effects. Equation-of-state[141,142] or lattice fluid theories[134,143,144] can often account for these features, but not necessarily in a transparent way.

If a blend is taken inside the binodal, it will phase separate to give two coexisting phases with compositions given by the coexistence curve at that temperature. Although the final thermodynamic state is the same, the mechanism by which the final state is approached depends on whether the system is initially quenched to an unstable or a metastable state. In the former case, the phase separation is spontaneous, and the mechanism is termed spinodal decomposition. Starting from a metastable state results in nucleation and growth. These two processes are illustrated schematically in Figure 17.[145]

In spinodal decomposition, the time evolution of composition is obtained from the continuity equation[11,146]

$$\partial\phi(\vec{r},t)\partial t = -\nabla\cdot\vec{J} \tag{3.13}$$

where $\vec{J}$ is the flux, given by

$$\vec{J} = -\frac{\Lambda}{kT}\nabla\mu \tag{3.14}$$

with $\nabla\mu$ being the chemical potential gradient at $\vec{r}$; Λ, the Onsager coefficient, is the mobility. In general, Λ is nonlocal in view of the appreciable physical size of polymer molecules; it is a function of N_1, N_2, ϕ, and the self diffusion coefficients. The chemical potential is obtained from eq 3.4 or 3.8. Therefore, eq 3.13 is highly nonlinear and is solved numerically. In the early stages, a linear stability analysis can be performed.[11,146] Using eq 3.11, eq 3.13 gives, for early times,

$$\frac{\partial}{\partial t}\Delta\psi(q,t) = -\Lambda q^2(A + \kappa q^2)\Delta\psi(q,t) + ... \tag{3.15}$$

where $A < 0$ in the spinodal region. Therefore, the fluctuations and $S(q,t)$ depend on time exponentially,

$$S(q,t) \sim \exp\{-\Lambda q^2(A+ \kappa q^2)t\} \tag{3.16}$$

so that large wavelength fluctuations with $q \le q_c = \sqrt{|A|/\kappa}$ grow with time, while small wavelength fluctuations, with $q \ge q_c$, decay. This spontaneous selection of large wavelength fluctuations establishes sufficient gradients for nonlinear effects to dominate. Due to the smallness of Λ and q_c, polymer blends are excellent experimental systems to investigate the early stage of spinodal decomposition.[144,147,148] In the intermediate stages of spinodal decomposition, the average domain size, R, increases as $t^{1/3}$, by either the Lifshitz−Slyozov evaporation−condensation or the coalescence mechanisms. In the late stages, hydrodynamic effects dominate, and $R \sim t$.

Systematic experiments on nucleation and growth in polymer blends have only recently begun.[149,150] The theoretical description of this process considers the competition between the free energy gain associated with formation of a droplet of the equilibrium phase and the free energy loss accompanying the creation of the droplet surface, as with small molecules. Droplets with a larger than critical radius grow, whereas smaller droplets redissolve. If critical droplets are formed by thermal fluctuations in the metastable state, the process is termed homogeneous nucleation. If the surface for growth is provided by impurities such as dust particles or residual catalyst, then the process is called heterogeneous nucleation; this is always dominant in practical situations. The late stage of nucleation and growth is presumed to be similar to that of spinodal decomposition. The droplet model of nucleation can also be used in understanding crystallization of polymers from liquid phases. In this case, the morphology of crystalline polymers is extremely rich and is very different from spherical droplets.[151]

4. Interfaces and Tethered Chains

4.A. General Features. A surface or interface imposes both entropic and energetic constraints, the effects of which can persist tens of nanometers into a bulk phase. For example, a hard surface removes conformational degrees of freedom for any flexible chain whose center of mass is within *ca.* R_g of the wall. This can lead to a polymer depletion zone for solutions near the walls of pores and favors migration of shorter polymers to the free surface of a melt. In the stiff chain limit, a hard surface can induce liquid crystalline order. From an energetic perspective, polymers with lower surface energies, Γ, will preferentially segregate to the surface. Thus, in a miscible polymer blend, the surface will be enriched in one component, at the cost of mixing entropy. The result is a composition profile that decays to the bulk average over length scales of order R_g. Functional groups on polymers, or simply chain ends, can also preferentially locate in the near surface region, with a myriad of potential applications for tailoring the properties of material surfaces. In many situations, polymers have one monomer anchored to a surface or interface; these are termed "tethered chains".[152]

4.B. Polymer Brushes. A "brush" is a dense layer of chains that are grafted to a surface or interface; "dense" in this context means that the average distance between tethering points is much less than the unperturbed dimensions of the chain.[152] As a consequence of this crowding, the chains stretch away from the surface, incurring an entropic penalty. The balance between osmotic and elastic contributions dictates the free energy, composition profile, and spatial extent of the brush. Brushes arise in a variety of interesting circumstances, including grafted layers, colloidal stabilization, highly branched polymers, micelles, and block copolymer microstructures.

Consider a planar surface (see Figure 18) to which are anchored chains of N segments, with a mean separation of anchors $d \ll N^{1/2}b$; the areal density of chains, σ, is thus d^{-2}. (If $N^{1/2}b \le d$, the chains can ignore each other, in a situation referred to as "mushrooms".) In the simplest, mean-field limit, the layer composition profile is assumed to be a step function of height L, with constant polymer volume fraction $\phi = Nb^3/Ld^2$.[153,154] The free energy may be estimated as a balance of

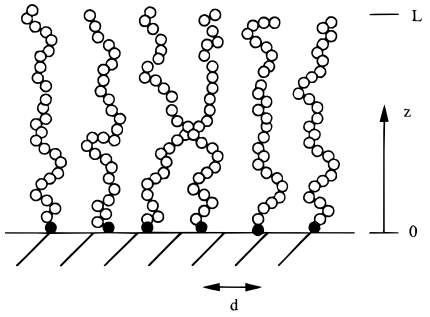

Figure 18. Schematic illustration of a grafted layer or brush.

excluded volume and elastic forces (*cf.* eq 2.4):

$$\frac{F}{kT} = w\phi^2 d^2 \frac{L}{b} + \frac{L^2}{Nb^2} \tag{4.1}$$

where the first term penalizes monomer−monomer contacts and the second distortion of the coil. Minimization with respect to L gives

$$\frac{L}{b} \sim w^{1/3} N \left(\frac{b}{d}\right)^{2/3} \tag{4.2}$$

The interesting result is that the layer height scales linearly with N, in contrast to the untethered equivalent, where $R_g \sim N^{3/5}$. This mean-field treatment of F suffers from some of the same limitations as in solutions but nevertheless produces the correct scaling of L with N. This scaling persists in a theta solvent, where $w = 0$. The appropriate F reflects three-body interactions, $F_{ex} = v\phi^3 d^2 L/b^3$ (*cf.* eq 2.6), with the result

$$\frac{L}{b} \sim v\, N \frac{b}{d} \tag{4.3}$$

The treatment of F may be improved with a blob approach, as in section 3.A; however, the main difficulty is the assumption of a uniform density profile. An SCF approach offers a means to determine $\phi(z)$ more precisely. An appealing analogy was drawn by Semenov:[155] a weakly stretched or unstretched chain follows a trajectory identical in form to that of a quantum particle (*i.e.*, a solution to the Schrödinger equation; *cf.* eq 1.2), whereas in the limit of complete stretching, the chain follows a "classical" trajectory (*i.e.*, a solution to Newton's law). Consequently, for strongly stretched chains the SCF allows fluctuations about this most probable trajectory. If one begins the trajectory at the free end of each chain, no matter what the conformation, the chain has N "steps" to arrive at the surface ($z = 0$), beginning with zero "velocity". The field of surrounding monomers provides a potential, which must be an "equal time", or harmonic, potential. (A ball placed at random in a harmonic well, with zero initial velocity, will first reach the bottom at a time independent of initial position.) Thus, the composition profile is parabolic:[156,157]

$$\phi(z) \sim (z^2 - L^2) \tag{4.4}$$

and it is a necessary condition that the chain end distribution be nonvanishing throughout the brush. Note, however, that $L \sim N$ as before. This profile has some experimental support, as well as close agreement with computer simulation.[152]

These arguments have been extended to curved surfaces, such as occur in micelles[155] or highly branched polymers.[158] Generally, stretching is reduced relative to the planar grafting surface, as further from the interface there is more space to relieve crowding. In the mean-field limit, $R \sim N^{3/4}$ for a cylindrical grafting surface and $R \sim N^{3/5}$ for a spherical object.

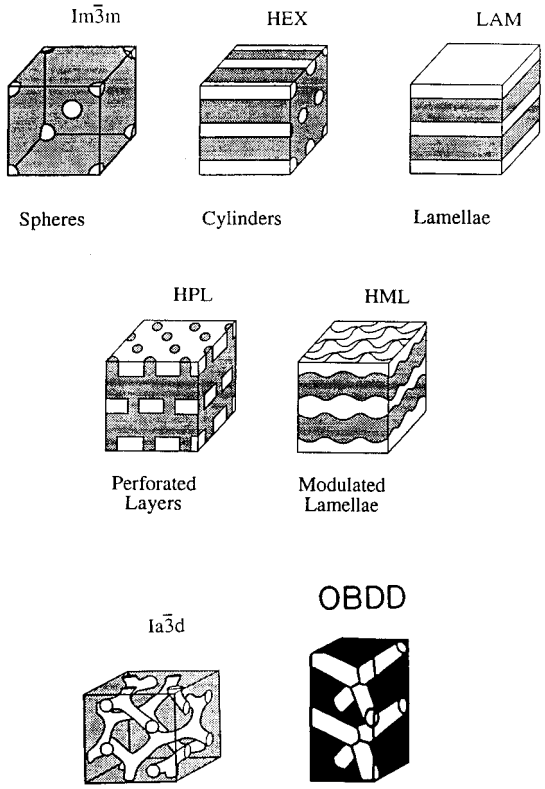

Figure 19. Experimentally assigned morphologies for diblock copolymers.[171]

4.C. Block Copolymer Microstructures. Block copolymers comprise two or more sequences of distinct units covalently linked together, *e.g.*, ...AAAAAA−BBBBB... The composition variable is $f_A = N_A/(N_A + N_B)$. The A/B interactions drive the system to self-assemble into a variety of morphologies, in a manner reminiscent of small molecule surfactants. However, the length scales associated with such structures are governed by the chain size and are typically in the 10−100 nm range. Copolymers are of technological importance, because the covalent linkage prevents macroscopic phase separation; a stable material with both A-like and B-like character can be produced, or copolymers can be used to compatibilize polymer blends.[159−164]

For a given molecule and temperature, the central questions are (a) what is the equilibrium morphology, (b) what is the composition profile, and (c) how does the periodicity scale with χ and N? Theoretical treatments of block copolymer microstructures were first developed for two limiting regimes, designated "strong" and "weak" segregation, according to whether the enthalpic terms dominate the free energy or not. In strong segregation ($\chi N >$ *ca.* 50),[155,165,166] A/B contacts are very expensive, and so the system seeks narrow interfacial profiles and a low interfacial area per unit volume. Consequently, one may assume a step function concentration profile, and the preferred morphologies are lamellar ($0.30 < f < 0.50$), hexagonal ($0.12 < f < 0.30$), and body-centered cubic (space group $Im\bar{3}m$) ($0 < f \leq 0.12$) (see Figure 19). To locate boundaries between morphologies, one must evaluate free energies for a given set of postulated structures; the structure is not a consequence of the calculation. More detailed SCF calculations give precise locations of these boundaries, plus the deviation from step-function interfaces.[167] The approximate dependence of the periodicity, L, on χ and N can be obtained simply from an enthalpy/entropy balance, as before. The

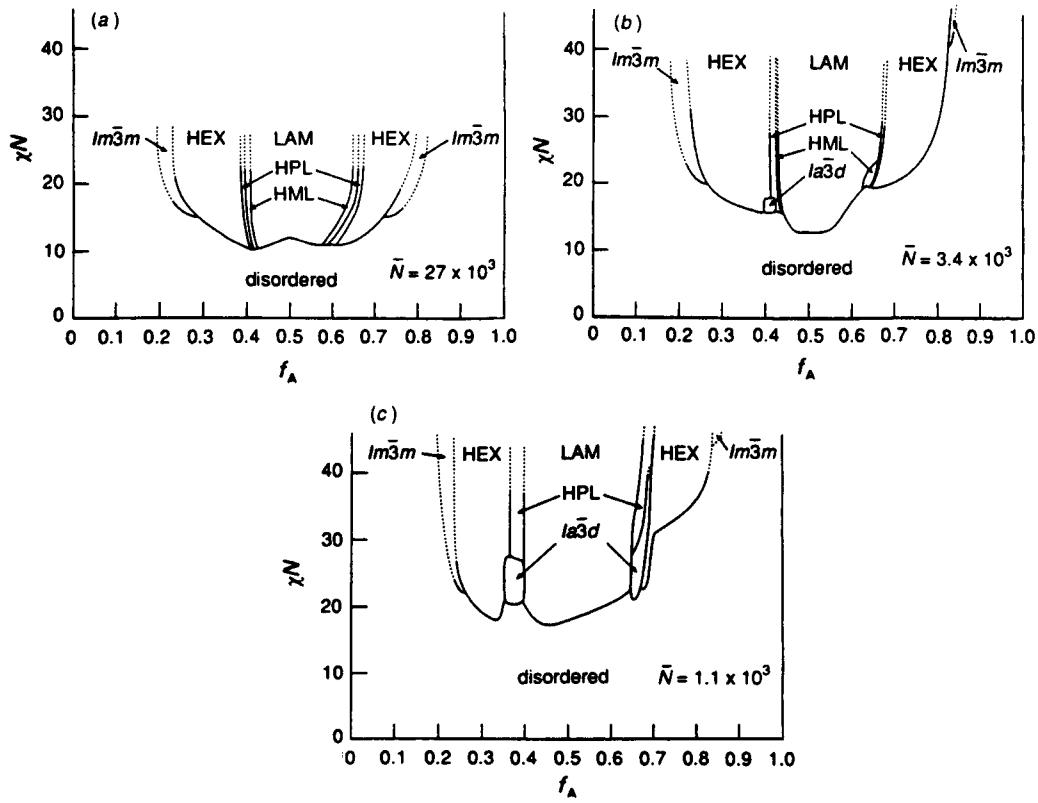

Figure 20. Phase diagrams for four different copolymer systems: (a) polyethylene−poly(ethylenepropylene), (b) poly(ethylenepropylene)−poly(ethylethylene) and polyethylene−poly(ethylethylene), and (c) polyisoprene−polystyrene. Reproduced with permission from ref 171. Copyright 1994 Royal Society of Chemistry.

minimum interfacial area would have each junction point confined to a thin surface, with the chains stretched out completely to fill space and maintain bulk density; however, this chain stretching is entropically prohibitive. The interfacial energy per chain is (Γ)(area/chain) ~ $\Gamma N/\rho L$,whereas the stretching entropy is taken, as usual, to be $\sim L^2/Nb^2$. The net result is therefore (using eq 3.9)

$$L \sim N^{2/3}\Gamma^{1/3} = N^{2/3}\chi^{1/6} \tag{4.5}$$

This stretching is much weaker than in a grafted layer, due to the ability of the copolymers to adjust their "grafting" density. All of these strong segregation results have good experimental support, particularly from the pioneering work of Hashimoto and co-workers.[163,168]

In weak segregation, one is concerned with the location of the first appearance of a periodic structure at the order−disorder transition (ODT). Leibler employed a (mean-field) Landau expansion of the free energy to locate the ODT at $\chi N \approx 10.5$ for $f = 0.5$.[169] In this analysis, it is assumed that the composition profile is sinusoidal, with vanishing amplitude at the ODT for $f = 0.5$ and that the chains are unstretched ($L \sim N^{1/2}b$). The free energies of different periodic structures are compared by appropriate evaluation of the coefficients in the expansion. In Leibler's original paper, the transition was predicted to be into the bcc phase at all asymmetric compositions ($f \neq 0.5$), which is not the case experimentally. However, this difficulty can be removed by including higher Fourier harmonics in the free energy calculation for a given structure (*i.e.*, lifting the assumption of sinusoidal profiles)[167] and/or by including fluctuation effects.[170] These fluctuations stabilize the disordered state and allow direct, weakly first-order transitions into the lamellar and hexagonal microphases, as has been observed experimentally.[171] The detailed description of these fluctuations remains somewhat controversial,[170,172−174] but their origin is qualitatively easy to understand. For a symmetric homopolymer blend ($N_A = N_B = N$, $\phi_A = \phi_B$), the critical point occurs at $(\chi N)_c = 2$, whereas if one links these two chains at their ends, the ODT does not occur until $\chi(N_A + N_B) \approx 10.5$. There is thus a wide range of temperature ($4 < \chi(N_A + N_B) < 10.5$) over which the two blocks "feel" a desire to segregate. This may be accomplished on a local scale by transient regions of nonuniform composition. The periodicity of these fluctuations must scale approximately as R_g and correspond to a peak in $S(q)$ at $q^* \sim 1/R_g$. The segregation is quite subtle, however; for example, it might be accomplished by chain stretching (separation of the centers of mass of the two blocks) with or without modification of the Gaussian distribution within one block.

Early experimental work in this area centered on styrene−diene copolymers, which typically were strongly segregated.[163] The spherical, hexagonal, and lamellar phases were found and examined in some detail. The interfacial thickness was extracted, and the domain period scaled as $N^{2/3}$.[168] The boundaries between morphologies along the composition axis were also roughly in accordance with theory. One provocative new structure was observed in a narrow composition window between the hexagonal and lamellar phases.[175] It was assigned as the ordered bicontinuous double diamond (OBDD, space group $Pn\bar{3}m$; see Figure 19) largely on the basis of electron microscopy.[176] It was not found to be the low-energy state in free energy calculations, however.[167,177] More recently, there have been extensive examinations of a wider variety of chemical structures, in both weak and intermediate segregation regimes, with intriguing results.[171] First, three new bicontinuous morphologies appear between the hexagonal and lamellar structures: the "gyroid" (space group $Ia\bar{3}d$), hexagonally perforated layers ("catenoid lamellae"), and hexagonally modulated layers, as shown in Figure 19. All three experimental phase diagrams shown in Figure 20 are asymmetric about $f = 0.5$. In some

cases the asymmetry is such that the $Ia\bar{3}d$ phase appears only on one side of the diagram. This asymmetry has been attributed, in the main, to differences in chain conformation. For example, consider polyethylene and poly(ethylethylene). In the former, all carbon−carbon bonds lie along the backbone, whereas only half do in the latter. For equal molecular weights, the PE chain will be long and thin, with a large R_g, whereas the short, fat PEE block will be more compact. Consequently, the PE−PEE interface will be more likely to be concave toward the PEE domains. This amounts to a nonlocal entropic contribution to the free energy, which should also contribute in polymer blends.[178] The phase diagrams in Figure 20 also exhibit a dependence on N alone, in addition to that on the product χN, with the complexity increasing as N decreases. This is consistent with the general trend in polymers toward more mean-field behavior as N increases, so that fluctuation contributions diminish in importance, and it may be attributed in part to the packing difficulties associated with short segments in non-space-filling morphologies such as cylindrical micelles. Small molecule surfactants, for example, are well-known to exhibit a much richer array of phases than those of high molecular weight block copolymers.[179]

The dynamics of block copolymers may differ from their homopolymer counterparts in three general ways: structure, friction, and entanglement.[164] The first is the the most interesting and the most obvious: the interactions between A and B monomers drive segregation and produce periodic structures. In general, these structures can be expected to retard chain mobility, as the free energy landscape becomes more featured, leading to localization of chain junctions in interfacial regions. Furthermore, lamellar and hexagonal microphases may induce anisotropic motion. Strong rheological signatures of microphase formation may also be expected and are observed.[180−183] The second issue is the effective monomeric friction coefficient, ζ, for a copolymer. As is well-known from homopolymers, ζ is strongly T-dependent and structure-specific ($\tau_{seg} \sim \zeta b^2/kT$). However, once polymers are mixed, both ζ_A and ζ_B will depend on matrix composition, in a manner that is as yet little understood. For copolymers, one has the complication of a compositionally heterogeneous environment, such that ζ_A and ζ_B may be functions of position along the chain. Furthermore, ζ_A and ζ_B may differ by orders of magnitude from expectation based on an "ideal mixing" rule, so that, numerically this effect can swamp all others; these issues remain largely unexplored. The entanglement problem is not likely to be as important numerically, but still raises interesting issues.[184] What is the appropriate length scale for entanglement of a block copolymer? Is it possible for two blocks to have different entanglement length scales in a homogeneous mixture? If a chain is reptating, is it possible for the "tube" diameter to vary with position along the chain? These issues also await detailed examination.

The rheological properties of block copolymer melts have been examined in some detail.[164] In the linear viscoelastic limit, the frequency dependence of $G^*(\omega)$ in the low- and moderate-frequency regime varies markedly with morphology. The low-frequency regime, in which $G' \sim \omega^2$ and $G'' \sim \omega$ for simple liquids, exhibits interesting intermediate scalings, such as $G' \sim G'' \sim \omega^{1/2}$ for lamellae.[185] In the disordered state, but near the ODT, composition fluctuations can lead to a low frequency shoulder in the terminal regime, particularly in G'.[186] Cubic phases tend to exhibit broad plateaus in G', reminiscent of the entanglement plateau in homopolymer melts, but here attributable to the connectivity of at least one domain. In all cases the temperature dependence of G' in the low-frequency regime is an excellent diagnostic of the ODT or of order−order transitions

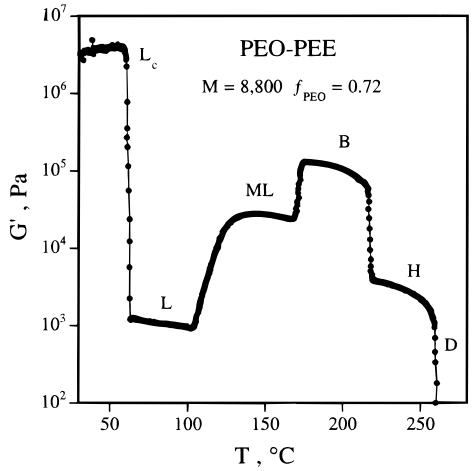

Figure 21. Shear elastic modulus for a poly(ethylene oxide)−poly(ethylethylene) diblock copolymer as a function of temperature.[187] The assigned morphologies are crystalline lamellar (L_c), amorphous lamellar (L), modulated lamellar (ML), bicontinuous cubic (B), hexagonal (H), and disordered (D).

when they occur; a spectacular example is shown in Figure 21, where a single copolymer exhibits five distinct ordered phases.[187] Comprehensive theoretical treatments of these various features of block copolymer viscoelasticity are lacking.[164]

Under large-amplitude strain, block copolymer microstructures can undergo alignment to generate "single-crystal"-like macroscopic structure.[188,189] Here also interesting features have emerged. For example, lamellae can orient with the lamellar normal along either the gradient ("parallel" orientation) or vorticity ("perpendicular" orientation) axes, depending on the choice of frequency, strain amplitude, and temperature relative to the ODT.[190−192] A full explanation of the phenomenology is not yet available, but some possible factors can be identified. The perpendicular orientation decouples the vorticity of the shear from the interfaces, which can resist deformation quite strongly. On the other hand, in systems with strong "viscoelastic contrast", *i.e.*, the viscosities of the two constituents are greatly different, the parallel orientation might be favored to distribute the deformation primarily in the less viscous layer. Entanglements and defect/grain boundary motion may also be implicated.[164]

4.D. Micelles. When a block copolymer is dispersed in a low molecular weight solvent (S), the structure and dynamics can be altered in profound ways. The principal new feature is the solvent selectivity, that is, the difference between χ_{AS} and χ_{BS}. If either is sufficiently large that the solvent does not dissolve that block, large aggregates or micelles will form, even at extremely low concentrations.[193,194] Such structures are of interest for a variety of reasons, including extraction, separation, and drug delivery systems. Or, if the copolymer is a symmetric triblock (ABA) and the solvent prefers the B units, the assembly of the A units can result in a transient network or gel. In the limit that $\chi_{AS} = \chi_{BS}$, the solvent is said to be neutral. Here, the solvent serves to disperse otherwise strongly segregated chains, *e.g.*, for processing advantages.

The critical micelle concentration (cmc), spatial extent, and aggregation number of spherical micelles in a selective solvent can be predicted, using a balance of terms similar to that encountered in block copolymer melts and grafted layers.[195,196] For a significantly asymmetric copolymer (*e.g.*, $f_A \gg f_B$) well above the cmc, two simple limits obtain.[197] If the A block does not dissolve, one anticipates a "crew-cut" micelle: the corona block, B, is very short. Or, if B does not dissolve, a star-like or "hairy" micelle with long corona chains results (see Figure 22). In the large χ_{AB} limit there will be a sharp core−corona

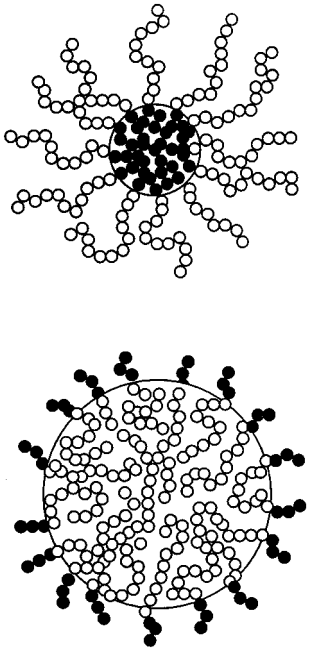

Figure 22. Schematic illustration of "hairy" and "crew-cut" micelles.

interface. The core radius is dictated by the aggregation number, f, and the bulk density of that component (assuming no solvation): $R_{core} = b(fN_{core})^{1/3}$. The energy of the interface scales as R_{core}^2/f, the surface area per chain. Both core and corona blocks are stretched, with corresponding entropic penalties $\sim(R_{core}^2/N_{core}b^2)$ and $f^{1/2}\ln(R/R_{core})$, respectively. For crew-cut micelles, the core contribution outweighs that from the corona, and minimization of $F_{int} + F_{core}$ gives

$$f = (\Gamma b^2)N_{core}; \quad R \approx N_{core}^{2/3} b \tag{4.6}$$

For the hairy micelle, F_{corona} competes with F_{int} to give

$$f = (\Gamma b^2)^{6/5} N_{core}; \quad R \approx N_{core}^{4/25} N_{corona}^{3/5} b \tag{4.7}$$

An interesting prediction of this anaysis is that aggregation numbers are determined entirely by the length of the insoluble block.

Block copolymer micelles have been the subject of intense experimental investigation for over 30 years.[193,194] However, these predictions have not been rigorously tested. Difficulties include preparation of a series of samples with constant N_{core}, sufficiently large χ_{AB} that the narrow interface approximation holds, sufficiently large χ between core and solvent that the core is not swollen, choice of nonglassy core blocks (*e.g.*, not PS or PMMA) so that equilibration is possible, and the need for labeled materials so that SANS can be used to resolve R_{core} and R_{corona}.

5. Summary and Future Prospects

5.A. Summary. Long polymer chains possess substantial conformational entropy, that in the absence of monomer−monomer interactions leads to a characteristic random walk scaling of chain size with molecular weight: $R_g \sim M^\nu$, with $\nu = {}^1/_2$. Excluded volume interactions in a good solvent cause the chain to swell and $\nu = 0.588$, whereas in a poor solvent, the coils can collapse and $\nu = {}^1/_3$. Alternatively, chains that are stiff can exhibit effective exponents that approach the rod limit of 1. The stiffness may originate in local steric constraints or from strong interactions, such as electrostatic repulsion between like charges on a polyelectrolyte. Strong interactions can also lead to entropic frustration: chains become trapped in conformations that correspond to deep local minima in phase space.

The chain trajectory may be described by a diffusion equation, with the addition of a potential term that requires a self-consistent solution. The enthalpic interactions embodied in this potential compete with the entropic drive toward randomness to establish the equilibrium average conformation. This approach is particularly powerful in describing "tethered" chains: polymers in which one monomer is confined to an interface. Steric crowding of tethered chains produces a "brush": chains stretch away from the interface to reduce unfavorable monomer−monomer contacts. This produces new values of the size exponent, *e.g.*, $\nu = {}^2/_3$ for strongly segregated block copolymers and $\nu = 1$ for chains anchored to a planar interface. Interfaces also reduce conformational entropy in the absence of tethering, leading to near-surface segregation effects that decay over length scales on the order of R_g.

The dynamics of flexible chains are often modeled successfully with systems of "beads"—point sources of friction with the environment—connected by elastic "springs"—representing the entropy of flexible chain segments. However, such idealizations break down at short time scales, when local structural details become important, and at high rates of strain. In dilute solution the dynamic properties are rather well understood; the dominant force on a chain segment, beyond the frictional and spring forces, is due to through-space hydrodynamic interactions among all the segments. In melts chain uncrossability leads to the phenomenon of entanglement, whereby long chains behave as though subject to long-lived, transient cross-links. The reptation model provides the most successful treatment of dynamics in this regime, but significant questions persist. Furthermore, the crossover from semidilute solution to entangled chain dynamics remains controversial.

Polymer mixtures, particularly copolymers and blends, combine thermodynamics and dynamics in ways that have both broad fundamental and technological implications. Although mean-field theory provides a successful framework for interpreting the phenomenology, quantitative free energy calculations are generally discouragingly complicated. Both of these feaures reflect the large molecular size: many interaction sites per molecule make mean-field theory more relevant but magnify the effect of any uncertainty in computing the local interactions. The time evolution of structure in phase separating systems remains a fertile area, particularly for asymmetric mixtures and blends with copolymer additives. Block copolymer melts continue to provide morphological surprises, and their rich dynamic properties are just beginning to be explored.

5.B. Future Prospects. A recent report examines the state of polymer science and engineering in both breadth and detail, with a particular view toward identifying areas for future research emphasis, based primarily on their connections to issues of national importance.[1] Specific recommendations are offered about advanced technological applications, materials processing, synthesis, characterization, theory, and simulations. These reflect the wisdom and input of a wide range of scientists and engineers. Our comments below have a rather different perspective. First, we are much more narrowly concerned with problem areas of potential interest to physical chemists, although we encourage a broad definition of that discipline. Second, we are not charged with strategic or economic concerns and can concentrate entirely on the underlying science. However, it is one of the great virtues of polymer physical chemistry that the distance between fundamental science and technological application is rarely very great. Third, rather than offer specific

recommendations, we cater to our own prejudices and simply identify five broad, interwoven themes that we expect to figure prominently in the near future.

(i) Polymers as Model Thermodynamic Systems. Polymers afford unique opportunities for detailed study of the thermodynamics of "soft" condensed matter, such as self-assembly processes and phase transitions. There are at least five reasons for this. First, polymers, by virtue of their molecular size, tend to be more amenable to mean-field analysis. Second, interaction strengths may be tuned with exquisite resolution, through control of either molecular weight or chemical structure. Third, the natural length scales are ideally suited to quantitative analysis by scattering and, increasingly, by microscopy. Fourth, the inherently long relaxation times permit monitoring of complicated kinetic processes in full detail. Fifth, the evolving microstructures are often sufficently robust that they may be quenched, for example for off-line structural analysis.

(ii) Bridging the Gap between Nanoscale and Microscale. Materials with precise two- or three-dimensional structures tend to be assembled from atomic or small molecule constituents, with features on the 1−10 Å scale, or processed from the bulk, with resolution on the 0.1−1 μm scale. Polymers naturally bridge this gap, as their characteristic dimensions lie in the 10−10^3 Å range. Block copolymers, blends, and semicrystalline and liquid crystalline polymers are all examples of systems which can form controlled morphologies in this regime. The thermodynamic factors that underlie a given equilibrium morphology generally feature a subtle competition between entropic and energetic terms, while kinetic considerations bring in all the complexity of cooperative chain dynamics. Sophisticated theoretical analysis of such materials under processing conditions presents an important challenge.

(iii) Biological Paradigm I: Increased Control of Molecular Architecture. Free radical copolymerization and biological synthesis of proteins represent extremes in the preparation of polymer materials. In the former, there is little control over chain length, chain length distribution, composition, monomer sequence, or sterochemistry of addition, whereas in the latter, nature draws from a pool of 20 monomers and exerts precise control over the addition of every unit. A major current focus of polymer synthetic chemistry is to emulate nature to a greater degree and particularly in the control of sequence. Although this might appear to lie outside the province of physical chemistry, it does not; the design of appropriate target molecules, "heteropolymers" with particular functionalities in particular locations, depends on clear ideas for desired properties. For example, efficient imitation of sophisticated biological functions by synthetic polymers will require explicit models for a minimal set of necessary molecular attributes. The statistical mechanics of nonergodic systems will play an increasingly important role.

(iv) Biological Paradigm II: Functional Soft Materials through Multiple Interactions. Biological systems often function through a delicate balance among different interactions—hydrogen bonding, hydrophobic/hydrophilic domains, partially screened electrostatics, acid/base functionalities—whereas a given synthetic polymer exhibits only one or two nonspecific interactions. One consequence of the multiple interaction approach is the ability of biological systems to generate strong responses to weak stimuli in very selective ways. Synthetic "soft" materials—gels, copolymers, liquid crystals, surfactant mixtures—offer rich opportunities for developing molecular systems with the sophistication of their biological counterparts, but ultimately with superior efficiency, due to prior selection of a limited set of target functions.

(v) Interfacial Properties and the Transition from Two to Three Dimensions. Many applications of polymers rely on interfacial properties; adhesives, coatings, and surfactants are obvious examples. Yet, only recently has a molecular understanding of polymers near surfaces progressed rapidly. Polymers are rarely strictly confined to two dimensions, as molecular size guarantees that effects of a surface are felt tens to hundreds of angstroms away. There are thus many "bulk" polymers, block copolymers being a prime example, for which the majority of the material is interfacial in character, and the resulting properties are not simply reflective of either two- or three-dimensional materials. Recent work has emphasized structural features along the direction normal to the surface, and rather little is known about the control of in-plane molecular arrangement or pattern formation. Such control could open new horizons in the preparation of tailored surfaces and interfaces; the function of a cell membrane provides another relevant biological paradigm. The design of interfaces between polymers and other classes of materials—metals, semiconductors, ceramics—also promises to be a fruitful area.

Acknowledgment. We would like to thank F. S. Bates and M. Tirrell for illuminating discussions and M. Hillmyer for providing one of the figures.

References and Notes

(1) *Polymer Science & Engineering: The Shifting Research Frontiers*; National Academy Press: Washington, DC, 1994.
(2) Flory, P. J. *Principles of Polymer Chemistry*; Cornell University Press: Ithaca, NY, 1953.
(3) Volkenstein, M. V. *Configurational Statistics of Polymeric Chains*; Interscience: New York, 1963.
(4) Flory, P. J. *Statistical Mechanics of Chain Molecules*; Interscience: New York, 1969.
(5) Yamakawa, H. *Modern Theory of Polymer Solutions*; Harper & Row: New York, 1971.
(6) de Gennes, P. G. *Scaling Concepts In Polymer Physics*; Cornell University Press: Ithaca, NY, 1979.
(7) Doi, M.; Edwards, S. F. *The Theory of Polymer Dynamics*; Clarendon Press: Oxford, 1986.
(8) des Cloizeaux, J.; Jannink, G. *Polymers in Solution*; Clarendon Press: Oxford, 1990.
(9) Freed, K. F. *Renormalization Group Theory of Macromolecules*; Wiley: New York, 1987.
(10) Fujita, H. *Polymer Solutions*; Elsevier: New York, 1990.
(11) Muthukumar, M.; Edwards, S. F. In *Comprehensive Polymer Science*; Booth, C., Price, C., Eds.; Pergamon Press: Oxford, 1989; Vol. 2, p 1.
(12) More properly, the local stiffness is characterized by a persistence length, which is closely related to, but logically distinct from, the statistical segment length. However, the latter is more useful in computing flexible chain dimensions and will be used exclusively throughout the paper.
(13) Edwards, S. F. *Proc. Phys. Soc., London* **1965**, *85*, 813.
(14) Debye, P. *J. Phys. Colloid Chem.* **1947**, *51*, 18.
(15) Stauffer, D.; Aharony, A. *Introduction to Percolation Theory*; Taylor & Francis: London, 1992.
(16) Muthukumar, M. *J. Chem. Phys.* **1996**, *104*, 691.
(17) Muthukumar, M. *J. Chem. Phys.* **1995**, *103*, 4723.
(18) Szwarc, M. *Carbanions, Living Polymers and Electron Transfer Processes*; Interscience: New York, 1968.
(19) Morton, M.; Fetters, L. J. *Rubber Chem. Technol.* **1975**, *48*, 359.
(20) Webster, O. W. *Science (Washington, D.C.)* **1991**, *251*, 887.
(21) Webster, O. W.; Hertler, W. R.; Sogah, D. Y.; Farnham, W. B.; Rajanbabu, T. V. *J. Am. Chem. Soc.* **1983**, *105*, 5706.
(22) Wagener, K. B.; Boncella, J. M.; Nel, J. G. *Macromolecules* **1991**, *24*, 2649.
(23) Schrock, R. R. *Acc. Chem. Res.* **1990**, *23*, 158.
(24) Grubbs, R. H.; Gilliom, L. R. *J. Am. Chem. Soc.* **1986**, *108*, 733.
(25) Miyamoto, M.; Sawamoto, M.; Higashimura, T. *Macromolecules* **1984**, *17*, 265.
(26) Kennedy, J. P.; Marechal, E. *Carbocationic Polymerization*; Wiley: New York, 1982.
(27) Greszta, D.; Mardare, D.; Matyjaszewski, K. *Macromolecules* **1994**, *27*, 638.
(28) Helfand, E. In *Polymer Compatibility and Incompatibility*; Solc, K., Ed.; Harwood Academic Publishers: New York, 1982.

(29) Amit, D. J. *Field Theory, the Renormalization Group and Critical Phenomena*; McGraw-Hill: New York, 1978.
(30) Itzykson, C.; Drouffe, J.-M. *Statistical Field Theory*; Cambridge Unversity Press: Cambridge, 1989.
(31) Muthukumar, M. *Macromolecules* **1993**, *26*, 5259.
(32) Heerman, D. W. *Introduction to Computer Simulation Methods in Theoretical Physics*; Springer: Berlin, 1986.
(33) Baumgärtner, A. In *Applications of the Monte Carlo Method in Statistical Physics*; Binder, K., Ed.; Springer-Verlag: Berlin, 1984.
(34) Fisher, M. E. *J. Chem. Phys.* **1966**, *44*, 616.
(35) Domb, C.; Joyce, G. S. *J. Phys. C* **1972**, *5*, 956.
(36) Barrett, A. J.; Domb, C. *Proc. R. Soc. London, Ser. A* **1979**, *367*, 143.
(37) Barrett, A. J.; Domb, C. *Proc. R. Soc. London, Ser. A* **1981**, *376*, 361.
(38) Carmesin, I.; Kremer, K. *Macromolecules* **1988**, *21*, 2819.
(39) Metropolis, N.; Rosenbluth, A. W.; Rosenbluth, M. N.; Teller, A. N.; Teller, E. *J. Cherm. Phys.* **1953**, *21*, 1087.
(40) Lal, M. *Mol. Phys.* **1969**, *17*, 57.
(41) Madras, N.; Sokal, A. D. *J. Stat. Phys.* **1988**, *50*, 109.
(42) Alder, B. J.; Wainwright, T. E. *J. Chem. Phys.* **1960**, *33*, 1439.
(43) McCammon, J. A.; Harvey, S. C. *Dynamics of Proteins and Nucleic Acids*; Cambridge University Press: Cambridge, 1987.
(44) Kremer, K.; Grest, G. *J. Chem. Phys.* **1990**, *92*, 5057.
(45) Helfand, E.; Wasserman, Z. R.; Weber, T. A. *Macromolecules* **1980**, *13*, 526.
(46) Lodge, T. P. *Mikrochim. Acta* **1994**, *116*, 1.
(47) Huglin, M. B. *Light Scattering From Polymer Solutions*; Academic Press: New York, 1972.
(48) Higgins, J. S.; Benoit, H. C. *Polymers and Neutron Scattering*; Clarendon Press: Oxford, 1994.
(49) Glatter, O.; Kratky, O. *Small Angle X-ray Scattering*; Academic Press: London, 1982.
(50) Hervet, H.; Léger, L.; Rondelez, F. *Phys. Rev. Lett.* **1979**, *42*, 1681.
(51) Mills, P. J.; Green, P. F.; Palmstrøm, C. J.; Mayer, J. W.; Kramer, E. J. *Appl. Phys. Lett.* **1984**, *45*, 958.
(52) Stejskal, E. O.; Tanner, J. E. *J. Chem. Phys.* **1965**, *42*, 288.
(53) Poo, M.-M.; Cone, R. A. *Nature* **1974**, *247*, 438.
(54) Berne, B. J.; Pecora, R. *Dynamic Light Scattering*; Wiley: New York, 1976.
(55) Chu, B. *Laser Light Scattering*, 2nd ed.; Academic Press: San Diego, 1991.
(56) Brown, W. *Light Scattering. Principles and Development*; Oxford University Press: Oxford, 1995.
(57) Russell, T. P. *Mater. Sci. Rep.* **1990**, *5*, 171.
(58) Penfold, J.; Thomas, R. K. *J. Phys.: Condens. Matter* **1990**, *2*, 1369.
(59) For most of the paper we utilize R_g as the characteristic molecular size, rather than the end-to-end distance, although the latter may be conceptually simpler. The radius of gyration has the advantage that it is definable for any molecular structure, and it is directly measurable by scattering experiments; however, both size parameters scale the same way with N or L.
(60) des Cloizeaux, J.; Conte, R.; Jannink, G. *J. Phys., Lett.* **1985**, *46*, L137.
(61) Muthukumar, M.; Nickel, B. G. *J. Chem. Phys.* **1987**, *86*, 460.
(62) Nickel, B. G. *Macromolecules* **1991**, *86*, 460.
(63) Casassa, E. F.; Berry, G. C. In *Comprehensive Polymer Science*; Booth, C. Price, C., Eds.; Pergamon Press: Oxford, 1989; Vol. 2, p 71.
(64) Lifshitz, I. M.; Grosberg, A. Y.; Khokhlov, A. R. *Rev. Mod. Phys.* **1978**, *50*, 683.
(65) de Gennes, P. G. *J. Phys., Lett.* **1975**, *36*, L55.
(66) de Gennes, P. G. *J. Phys., Lett.* **1978**, *39*, L299.
(67) Chu, B.; Wang, Z. *Macromolecules* **1989**, *22*, 380.
(68) Chu, B.; Wang, Z. *Macromolecules* **1988**, *21*, 2283.
(69) Poland, D.; Scheraga, H. A. *Theory of Helix-Coil Transitions in Biopolymers*; Academic Press: New York, 1970.
(70) Förster, S.; Schmidt, M. *Adv. Polym. Sci.* **1995**, *120*, 51.
(71) Odijk, T. *J. Polym. Sci., Polym. Phys. Ed.* **1977**, *15*, 477. Skolnick, J. A.; Fixman, M. *Macromolecules* **1977** *10*, 944.
(72) Manning, G. S. *Q. Rev. Biophys.* **1978**, *11*, 179.
(73) Bauer, B. J.; Fetters, L. J. *Rubber Chem. Technol.* **1978**, *51*, 406.
(74) Stockmayer, W. H.; Fixman, M. *Ann. N.Y. Acad. Sci.* **1953**, *57*, 334.
(75) Tomalia, D. A.; Baker, H.; Dewald, J.; Hall, M.; Kallos, G.; Martin, S.; Roeck, J.; Ryder, J.; Smith, P. *Macromolecules* **1986**, *19*, 2466.
(76) de Gennes, P. G.; Hervet, H. *J. Phys., Lett.* **1983**, *44*, L351.
(77) Lescanec, R. L.; Muthukumar, M. *Macromolecules* **1990**, *23*, 2280.
(78) Hammouda, B. *J. Polym. Sci., Polym. Phys. Ed.* **1992**, *30*, 1387.
(79) Mansfield, M. L.; Klushin, L. I. *J. Phys. Chem.* **1992**, *96*, 3994.
(80) Rouse, P. E., Jr. *J. Chem. Phys.* **1953**, *21*, 1272.
(81) Zimm, B. H. *J. Chem. Phys.* **1956**, *24*, 269.
(82) Bird, R. B.; Curtiss, C. F.; Armstrong, R. C.; Hassager, O. *Dynamics of Polymeric Liquids*, 2nd ed.; Wiley: New York, 1987; Vol. 2.
(83) Kirkwood, J. G.; Riseman, J. *J. Chem. Phys.* **1950**, *18*, 512.
(84) Lodge, A. S.; Wu, Y. *Rheol. Acta* **1971**, *10*, 539.
(85) Man, V. F.; Schrag, J. L.; Lodge, T. P. *Macromolecules* **1991**, *24*, 3666.
(86) Sammler, R. L.; Schrag, J. L. *Macromolecules* **1988**, *21*, 1132.
(87) Hair, D. W.; Amis, E. J. *Macromolecules* **1989**, *23*, 1889.
(88) Sammler, R. L.; Schrag, J. L. *Macromolecules* **1989**, *22*, 3435.
(89) Sahouani, H.; Lodge, T. P. *Macromolecules* **1992**, *25*, 5632.
(90) Lodge, T. P. *J. Phys. Chem.* **1993**, *97*, 1480.
(91) Gisser, D. J.; Ediger, M. D. *Macromolecules* **1992**, *25*, 1284.
(92) Krahn, J. R.; Lodge, T. P. *J. Phys. Chem.* **1995**, *99*, 8338.
(93) Schrag, J. L.; Stokich, T. M.; Strand, D. A.; Merchak, P. A.; Landry, C. J. T.; Radtke, D. R.; Man, V. F.; Lodge, T. P.; Morris, R. L.; Hermann, K. C.; Amelar, S.; Eastman, C. E.; Smeltzly, M. A. *J. Non-Cryst. Solids* **1991**, *131*−*133*, 537.
(94) Akcasu, A. Z.; Benmouna, M.; Han, C. C. *Polymer* **1980**, *21*, 866.
(95) *Dynamic Light Scattering: Applications of Photon Correlation Spectroscopy*; Pecora, R., Ed.; Plenum: New York, 1985.
(96) Nicholson, L. K.; Higgins, J. S.; Hayter, J. B. *Macromolecules* **1981**, *14*, 836.
(97) Martin, J. E.; Wilcoxon, J. P.; Odinek, J. *Macromolecules* **1992**, *25*, 4635.
(98) Han, C. C.; Akcasu, A. Z. *Macromolecules* **1981**, *14*, 1080.
(99) Sedlak, M.; Amis, E. J. *J. Chem. Phys.* **1992**, *96*, 817; 826.
(100) Lin, S. C.; Lee, W.; Schurr, J. M. *Biopolymers* **1978**, *17*, 1041.
(101) Schmitz, K. S.; Lu, M.; Gauntt, J. *J. Chem. Phys.* **1983**, *78*, 5059.
(102) Drifford, M.; Dalbiez, J. P. *Biopolymers* **1985**, *24*, 1501.
(103) Ise, N.; Yoshida, H. *Acc. Chem. Res.* **1996**, *29*, 3.
(104) Ferry, J. D. *Viscoelastic Properties of Polymers*, 3rd ed.; Wiley: New York, 1980.
(105) Flory, P. J. *J. Chem. Phys.* **1949**, *17*, 303.
(106) Kirste, R. G.; Kruse, W. A.; Schelten, J. *Makromol. Chem.* **1972**, *162*, 299.
(107) Wignall, G. D. In *The Encyclopedia of Polymer Science and Technology*; Wiley: New York, 1987; Vol. 10, p 112.
(108) Daoud, M. Ph.D. Thesis, Université de Paris VI, 1977.
(109) Daoud, M.; Cotton, J. P.; Farnoux, B.; Jannink, G.; Sarma, G.; Benoit, H.; Duplessix, R.; Picot, C.; de Gennes, P. G. *Macromolecules* **1975**, *8*, 804.
(110) King, J. S.; Boyer, W.; Wignall, G. D.; Ullman, R. *Macromolecules* **1985**, *18*, 709.
(111) Lodge, T. P.; Rotstein, N. A.; Prager, S. *Adv. Chem. Phys.* **1990**, *79*, 1.
(112) Tobolsky, A. V.; Catsiff, E. *J. Polym. Sci.* **1956**, *19*, 111.
(113) Treloar, L. R. G. *The Physics of Rubber Elasticity*; Clarendon Press: Oxford, 1975.
(114) Graessley, W. W.; Edwards, S. F. *Polymer* **1981**, *22*, 1329.
(115) Fetters, L. J.; Lohse, D. J.; Richter, D.; Witten, T. A.; Zirkel, A. *Macromolecules* **1994**, *27*, 4639.
(116) de Gennes, P. G. *J. Chem. Phys.* **1971**, *55*, 572.
(117) Berry, G. C.; Fox, T. G. *Adv. Polym. Sci.* **1968**, *5*, 261.
(118) Graessley, W. W. *Adv. Polym. Sci.* **1982**, *47*, 68.
(119) des Cloizeaux, J. *Europhys. Lett.* **1988**, *5*, 437.
(120) Higgins, J. S.; Roots, J. E. *J. Chem. Soc., Faraday Trans. 2* **1985**, *81*, 757.
(121) Richter, D.; Farago, B.; Fetters, L. J.; Huang, J. S.; Ewen, B.; Lartigue, C. *Phys. Rev. Lett.* **1990**, *64*, 1389.
(122) Kolinski, A.; Skolnick, J.; Yaris, R. *J. Chem. Phys.* **1987**, *86*, 7164, 7174.
(123) de Gennes, P.-G. *J. Phys. (Paris)* **1975**, *36*, 1199.
(124) Pearson, D. S.; Helfand, E. *Macromolecules* **1984**, *17*, 888.
(125) Klein, J. *Macromolecules* **1986**, *19*, 105.
(126) Ngai, K. L.; Rendell, R. W.; Rajagopal, A. K.; Teitler, S. *Ann. N.Y. Acad. Sci.* **1985**, *484*, 150.
(127) Kolinski, A.; Skolnick, J.; Yaris, R. *J. Chem. Phys.* **1988**, *88*, 1407, 1418.
(128) Schweizer, K. S. *J. Chem. Phys.* **1989**, *91*, 5802, 5822.
(129) Herman, M. F. *J. Chem. Phys.* **1990**, *92*, 2043.
(130) Huggins, M. L. *J. Chem. Phys.* **1942**, *46*, 151.
(131) Hill, T. L. *Introduction to Statistical Thermodynamics*; Addison-Wesley: Reading, MA, 1960.
(132) Kurata, M. *Thermodynamics of Polymer Solutions*; MMI Press: New York, 1982.
(133) Gehlsen, M. D.; Rosedale, J. H.; Bates, F. S.; Wignall, G. D.; Hansen, L.; Almdal, K. *Phys. Rev. Lett.* **1992**, *68*, 2452.
(134) Cahn, J. W.; Hilliard, J. E. *J. Chem. Phys.* **1959**, *31*, 668.
(135) Stanley, H. E. *Introduction to Phase Transitions and Critical Phenomena*; Oxford University Press: New York, 1971.
(136) Binder, K. *Phys. Rev. A* **1984**, *29*, 341.
(137) Bates, F. S.; Rosedale, J. H.; Stepanek, P.; Lodge, T. P.; Wiltzius, P.; Fredrickson, G. H.; Hjelm, R. P. *Phys. Rev. Lett.* **1990**, *65*, 1893.
(138) Schwahn, D.; Meier, G.; Mortensen, K.; Janssen, S. *J. Phys. II* **1994**, *4*, 837.
(139) Schwahn, D.; Mortensen, K.; Yee-Madeira, H. *Phys. Rev. Lett.* **1987**, *58*, 1544.

(140) Bates, F. S.; Wignall, G. D.; Koehler, W. C. *Phys. Rev. Lett.* **1985**, *55*, 2425.
(141) Sanchez, I. C. In *Encyclopedia of Physical Science and Technology*; Academic Press: New York, 1992; Vol. 13.
(142) Flory, P. J. *J. Am. Chem. Soc.* **1965**, *87*, 1833.
(143) Dudowicz, J.; Freed, K. F. *Macromolecules* **1991**, *24*, 5074.
(144) Binder, K. *J. Chem. Phys.* **1983**, *79*, 6387.
(145) Bates, F. S. *Science (Washington, D.C.)* **1991**, *251*, 898.
(146) Gunton, J. D.; San Miguel, M.; Sahni, P. S. In *Phase Transitions and Critical Phenomena*; Domb, C., Green, M. S., Eds.; Academic Press: London, 1983; Vol. 8.
(147) Han, C. C.; Akcasu, A. Z. *Annu. Rev. Phys. Chem.* **1992**, *43*, 61.
(148) Binder, K. *Adv. Polym. Sci.* **1994**, *112*, 181.
(149) Cumming, A.; Wiltzius, P.; Bates, F. S.; Rosedale, J. H. *Phys. Rev. A* **1992**, *45*, 885.
(150) Crist, B.; Nesarikar, A. R. *Macromolecules* **1995**, *28*, 890.
(151) Vaughan, A. S.; Bassett, D. C. In *Comprehensive Polymer Science*; Booth, C., Price, C., Eds.; Pergamon Press: Oxford, 1989; Vol. 2, p 415.
(152) Halperin, A.; Tirrell, M.; Lodge, T. P. *Adv. Polym. Sci.* **1991**, *100*, 33.
(153) Alexander, S. *J. Phys. (Paris)* **1977**, *38*, 977.
(154) de Gennes, P. G. *Macromolecules* **1980**, *13*, 1069.
(155) Semenov, A. N. *Sov. Phys. JETP* **1985**, *61*, 733.
(156) Zhulina, E. B.; Borisov, O. V.; Pryamitsin, V. A. *J. Colloid Interface Sci.* **1990**, *137*, 495.
(157) Milner, S. T.; Witten, T. A.; Cates, M. E. *Macromolecules* **1988**, *21*, 2610.
(158) Daoud, M.; Cotton, J. P. *J. Phys. (Paris)* **1982**, *43*, 531.
(159) *Block Copolymers*; Aggarwal, S. L., Ed.; Plenum: New York, 1970.
(160) *Block Copolymers: Science and Technology*; Meier, D. J., Ed.; MMI Press/Harwood Academic Publications: New York, 1983.
(161) *Developments in Block Copolymers-1*; Goodman, I., Ed.; Applied Science: New York, 1982.
(162) *Developments in Block Copolymers-2*; Goodman, I., Ed.; Applied Science: New York, 1985.
(163) Bates, F. S.; Fredrickson, G. H. *Annu. Rev. Phys. Chem.* **1990**, *41*, 525.
(164) Fredrickson, G. H.; Bates, F. S. *Annu. Rev. Mater. Sci.* **1996**, *26*, 503.
(165) Meier, D. J. *J. Polym. Sci. C* **1969**, *26*, 81.
(166) Helfand, E.; Wasserman, Z. R. *Macromolecules* **1976**, *9*, 879.
(167) Matsen, M. W.; Bates, F. S. *Macromolecules* **1996**, *29*, 1091.
(168) Hashimoto, T.; Shibayama, M.; Kawai, H. *Macromolecules* **1980**, *13*, 1237.
(169) Leibler, L. *Macromolecules* **1980**, *13*, 1602.
(170) Fredrickson, G. H.; Helfand, E. *J. Chem. Phys.* **1987**, *87*, 697.
(171) Bates, F. S.; Schulz, M. F.; Khandpur, A. K.; Förster, S.; Rosedale, J. H.; Almdal, K.; Mortensen, K. *J. Chem. Soc., Faraday Discuss.* **1994**, *98*, 7.
(172) Olvera de la Cruz, M. *J. Chem. Phys.* **1989**, *90*, 1995.
(173) Tang, H.; Freed, K. F. *J. Chem. Phys.* **1992**, *96*, 8621.
(174) David, E. F.; Schweizer, K. S. *J. Chem. Phys.* **1994**, *100*, 7767.
(175) Aggarwal, S. L. *Polymer* **1972**, *17*, 938.
(176) Thomas, E. L.; Alward, D. B.; Kinning, D. J.; Martin, D. C.; Handlin, D. L.; Fetters, L. J. *Macromolecules* **1986**, *19*, 2197.
(177) Likhtman, A. E.; Semenov, A. N. *Macromolecules* **1994**, *27*, 3103.
(178) Fredrickson, G. H.; Liu, A. J.; Bates, F. S. *Macromolecules* **1994**, *27*, 2503.
(179) Seddon, J. M. *Biochim. Biophys. Acta* **1990**, *1031*, 1.
(180) Chung, C. I.; Gale, J. C. *J. Polym. Sci., Polym. Phys. Ed.* **1976**, *14*, 1149.
(181) Gouinlock, E. V.; Porter, R. S. *Polym. Eng. Sci.* **1977**, *17*, 535.
(182) Widmaier, J. M.; Meyer, G. C. *J. Polym. Sci., Polym. Phys. Ed.* **1980**, *18*, 2217.
(183) Bates, F. S. *Macromolecules* **1984**, *17*, 2607.
(184) Rubinstein, M.; Obukhov, S. P. *Macromolecules* **1993**, *26*, 1740.
(185) Rosedale, J. H.; Bates, F. S. *Macromolecules* **1990**, *23*, 2329.
(186) Bates, F. S.; Rosedale, J. H.; Fredrickson, G. H. *J. Chem. Phys.* **1990**, *92*, 6255.
(187) Hillmyer, M. A.; Bates, F. S.; Almdal, K.; Mortensen, K.; Ryan, A. J.; Fairclough, P. A. *Science (Washington, D.C.)* **1996**, *271*, 976.
(188) Keller, A.; Pedemonte, E.; Willmouth, F. M. *Nature* **1970**, *225*, 538.
(189) Hadziioannou, G.; Mathis, A.; Skoulios, A. *Colloid Polym. Sci.* **1979**, *257*, 136.
(190) Koppi, K. A.; Tirrell, M.; Bates, F. S.; Almdal, K.; Colby, R. H. *J. Phys. II Fr.* **1992**, *2*, 1941.
(191) Kannan, R. M.; Kornfield, J. A. *Macromolecules* **1994**, *27*, 1177.
(192) Patel, S. S.; Larson, R. G.; Winey, K. I.; Watanabe, H. *Macromolecules* **1995**, *28*, 4313.
(193) Brown, R. A.; Masters, A. J.; Price, C.; Yuan, X. F. In *Comprehensive Polymer Science*; Booth, C., Price, C., Eds.; Pergamon Press: Oxford, 1989; Vol. 2.
(194) Tuzar, Z.; Kratochvil, P. In *Surface and Colloid Science*; Matijevic, E., Ed.; Plenum Press: New York, 1993; Vol. 15.
(195) Leibler, L.; Orland, H.; Wheeler, J. C. *J. Chem. Phys.* **1983**, *79*, 3550.
(196) Nagarajan, R.; Ganesh, K. *J. Chem. Phys.* **1989**, *90*, 5843.
(197) Halperin, A. *Macromolecules* **1987**, *20*, 2943.

JP960244Z